OPEN ACCESS

Original research

Engineered anti-PDL1 with IFNα targets both immunoinhibitory and activating signals in the liver to break HBV immune tolerance

Chao-Yang Meng,[1] Shiyu Sun,[1] Yong Liang,[2] Hairong Xu,[1] Chao Zhang ,[3] Min Zhang,[4] Fu-Sheng Wang ,[3] Yang-Xin Fu,[2] Hua Peng [1]

► Additional supplemental material is published online only. To view, please visit the journal online (http://dx.doi.org/10.1136/gutjnl-2022-327059).

For numbered affiliations see end of article.

Correspondence to
Professor Hua Peng, Key Laboratory of Infection and Immunity, Institute of Biophysics, Chinese Academy of Sciences, Beijing, China; hpeng@ibp.ac.cn
and Professor Yang-Xin Fu, Department of Basic Medical Sciences, School of Medicine, Tsinghua University, Beijing, China; yangxinfu@tsinghua.edu.cn

Received 28 January 2022
Accepted 12 October 2022
Published Online First 31 October 2022

ABSTRACT

Objective The purpose of this study is to develop an anti-PDL1-based interferon (IFN) fusion protein to overcome the chronic hepatitis B virus (HBV)-induced immune tolerance, and combine this immunotherapy with a HBV vaccine to achieve the functional cure of chronic hepatitis B (CHB) infection.

Design We designed an anti-PDL1-IFNα heterodimeric fusion protein, in which one arm was derived from anti-PDL1 antibody and the other arm was IFNα, to allow targeted delivery of IFNα into the liver by anti-PDL1 antibody. The effect of the anti-PDL1-IFNα heterodimer on overcoming hepatitis B surface antigen (HBsAg) vaccine resistance was evaluated in chronic HBV carrier mice.

Results The anti-PDL1-IFNα heterodimer preferentially targeted the liver and resulted in viral suppression, the PD1/PDL1 immune checkpoint blockade and dendritic cell activation/antigen presentation to activate HBsAg-specific T cells, thus breaking immune tolerance in chronic HBV carrier mice. When an HBsAg vaccine was administered soon after anti-PDL1-IFNα heterodimer treatment, we observed strong anti-HBsAg antibody and HBsAg-specific T cell responses for efficient HBsAg clearance in chronic HBV carrier mice that received the combination treatment but not in those that received either single treatment.

Conclusions Targeting the liver with an engineered anti-PDL1-IFNα heterodimer can break HBV-induced immune tolerance to an HBsAg vaccine, offering a promising translatable therapeutic strategy for the functional cure of CHB.

WHAT IS ALREADY KNOWN ON THIS TOPIC

⇒ High hepatitis B virus (HBV) antigen load and high level of programmed death ligand 1 (PDL1) in the liver lead to immune tolerance to HBV.
⇒ Type I interferon (IFN) is the most potent antiviral cytokine and can greatly enhance cross-presentation and T cell activation by dendritic cells (DCs). However, frequently repeated administration of IFN can cause systemic toxicity and induce PDL1 expression, which dampens the T cell response.
⇒ Without gaining protective immunity necessary to eradicate HBV, chronic hepatitis B (CHB) relapse is common after completion of antiviral therapy.

WHAT THIS STUDY ADDS

⇒ Anti-PDL1-IFNα heterodimer fusion protein, in which the affinity of anti-PDL1 to PDL1 is higher than IFNα to its receptor for better targeting IFNα into liver tissues.
⇒ Anti-PDL1-IFNα heterodimer can block immune checkpoint PDL1, target IFNα to the liver to suppress HBV replication and improve DC functions to break HBV immune tolerance.
⇒ Anti-PDL1-IFNα therapy combined with hepatitis B surface antigen (HBsAg) vaccination induced a strong and persistent anti-HBsAg immune response for CHB functional cure.

HOW THIS STUDY MIGHT AFFECT RESEARCH, PRACTICE OR POLICY

⇒ Anti-PDL1-IFNα combined with HBsAg vaccination can be a promising translatable therapeutic strategy for clinical CHB therapy and improve the clinical functional cure rate.

INTRODUCTION

Although effective prophylactic hepatitis B virus (HBV) vaccines have been available since the 1990s, an estimated 257 million people worldwide are living with chronic HBV infection, which poses a high risk for developing fibrosis, cirrhosis and hepatocellular carcinoma (HCC).[1 2] The functional cure of chronic hepatitis B (CHB), which is characterised by the loss of hepatitis B surface antigen (HBsAg) and HBV-DNA in the serum with seroconversion to anti-HBsAg, is a challenging endpoint for current CHB treatments to meet.[3–5] HBsAg seroclearance after anti-HBV therapy is associated with a significantly lower HCC incidence and mortality rate.[6] Type I interferons (IFNs), one type of approved drug, cannot effectively reduce the viral antigen load and hardly maintain sustained viral control after treatment withdrawal.[7 8] However, long-term repeated high-dose IFN treatment can cause systemic toxicity.[3] In addition, IFNs can upregulate the expression of the immunosuppressive molecule programmed death ligand 1 (PDL1), which in turn suppresses the antiviral immune response and gradually reduces the therapeutic effect.[9 10] The issue of how to overcome the systemic toxicity and

Linked

► http://dx.doi.org/10.1136/gutjnl-2022-328902

Check for updates

To cite: Meng C-Y, Sun S, Liang Y, *et al*. *Gut* 2023;**72**:1544–1554.

subsequent immunosuppression induced by IFNs remains to be solved.

The liver is an immunotolerant organ, especially in CHB patients. PDL1 is significantly upregulated in the liver of CHB patients, skewing the immune response towards the induction of tolerance in circulating naïve T cells and attenuating the effector functions of liver-infiltrating cytotoxic T lymphocytes (CTLs).[11 12] Conditional knockout of PDL1 in dendritic cells (DCs) can release these inhibitions, leading to better T cell activation.[13] To date, programmed death 1 (PD1)/PDL1 blockade therapy has been shown to induce an antitumour response in a small portion of patients with cancers.[14 15] In addition, several studies have reported that PD1/PDL1 blockade can partially restore HBV-specific T or B cell function in vitro.[16 17] However, the functional cure rate is fairly low in CHB patients receiving a PD1 inhibitor (nivolumab).[18] PD1/PDL1 inhibitors may enhance the ability of CTLs to kill infected hepatocytes, which can release many viruses to infect healthy hepatocytes. Killing infected cells while blocking viral reinfection is a challenge. High levels of viral antigens in the circulation, which impair DC and natural killer and HBV-specific T cell and B cell functions, abolish the host immunity needed to eradicate HBV.[16 19–21] T cells encounter HBV antigens poorly presented by DCs in the liver, which can lead to immune tolerance rather than functional activation.[22] We proposed that concurrent suppression of the viral load and enhancement of antigen presentation may be required to break tolerance for the induction of anti-HBV immunity.

We took advantage of the high expression of PDL1 in the liver of CHB patients and chronic HBV carrier mice and targeted IFNα with an anti-PDL1 antibody (anti-PDL1-IFNα) to simultaneously target PDL1 and type I IFN receptor (IFNAR) in the liver and thereby overcome local PDL1-mediated resistance and viral production. Importantly, the anti-PDL1-IFNα multifunctional fusion protein could overcome HBsAg vaccine resistance in chronic HBV carrier mice, produce strong anti-HBsAg neutralising antibody (NAb) and HBsAg-specific T cell responses, and achieve a functional cure of CHB in mice.

MATERIALS AND METHODS

Human samples

In this study, patient clinical information is listed in online supplemental table 1. Liver tissue samples were collected from healthy controls (HCs; n=6), non-HBV liver disease patients (n=3) and CHB patients (n=7) and stored by the Fifth Medical Center of Chinese PLA General Hospital (Beijing, China). Consent for collection of liver tissue samples was given by each patient in writing and authorised by the hospital ethics review committee.

Mice and an HBV carrier mouse model

- C57BL/6J mice (4–6 weeks old) were purchased from SiPeiFu (SPF) (Beijing) Biotechnology (Beijing, China). Rag1-deficient ($Rag1^{-/-}$) mice, which do not produce mature T cells and B cells, were purchased from the Model Animal Research Center of Nanjing University (Nanjing, China). $IFNAR1^{-/-}$ mice were kindly provided by Professor Haidong Tang (Tsinghua University, Beijing, China). Mice were maintained under specific pathogen-free conditions in an ABSL-2 animal facility, and animal experiments followed protocol Nos. DWSWAQ (ABSL-2) 2012205 and ABSL-2–201902 at the Institute of Biophysics, Chinese Academy of Sciences (Beijing, China) and were approved by the Biomedical Research Ethics Committee of the Institute of Biophysics of the Chinese Academy of Sciences.

The adeno-associated virus (AAV)-HBV1.3 virus was purchased from PackGene Biotech (Guangzhou, China). This recombinant virus carries 1.3 copies of the HBV genome (genotype D, serotype ayw) and is packaged in AAV serotype 8 capsids. Generation of the AAV/HBV carrier mouse model used in this study has been described previously.[23–26] Briefly, C57BL/6J mice were injected with the AAV-HBV1.3 virus through the tail vein (1×10^{11} viral genome copies per mouse). After 5 weeks or more, stable HBV carrier mice (serum HBsAg >1000 IU/mL) were used. Blood was collected from the retro-orbital sinuses at the indicated time points in the indicated experiments to monitor the levels of HBsAg, hepatitis B e antigen (HBeAg), ayw subtype-specific anti-HBsAg antibodies and HBV-DNA in the serum.

Fusion protein treatments and immunisation

To test the therapeutic effects of fusion proteins in vivo, HBV carrier mice were treated intravenously with 0.1687 nmol anti-PDL1-IFNα heterodimer two times with a 3-day interval. Other fusion proteins (anti-PDL1-IFNα homodimer, IFNα-Fc and anti-PDL1) were used to treat HBV carrier mice in the same manner with equimolar doses of IFNα and anti-PDL1 (as determined by the single subunit). Free IFNα (mouse IFNα4, His Tag) was purchased from Sino Biological (Beijing, China). A recombinant HBsAg (subtype ayw) protein with the same encoding sequence as that in AAV-HBV1.3 was purchased from Meridian Life Science Inc. (Memphis, USA) for vaccination and ex vivo stimulation assays. CpG-1826 (TCCATGACGTTCCTGACGTT), an adjuvant, was synthesised by Shanghai Generay Biotech (Shanghai, China). Two micrograms of recombinant HBsAg (subtype ayw)/30 μg CpG-1826 was used for subcutaneous immunisation at the indicated time points. Anti-CD4 (clone GK1.5) and anti-CD8 (clone TIB210) depleting antibodies were produced in-house. For $CD4^+$ and $CD8^+$ T cell depletion, HBV carrier mice were injected intraperitoneally with 200 μg anti-CD4 (GK1.5) and 200 μg anti-CD8 (TIB210) twice per week beginning 1 day before anti-PDL1-IFNα heterodimer treatment.

Statistical analysis

Data were analysed using an unpaired two-tailed Student's t-test with GraphPad Prism statistical software. Data are shown as the mean±SEM or mean+SEM. Statistically significant differences of $p<0.05$, $p<0.01$, $p<0.001$ and $p<0.0001$ are noted as *, **, *** and ****, respectively.

More details of the production of anti-PDL1-IFNα fusion proteins, detection of HBV markers, immunohistochemistry, flow cytometry analysis and enzyme-linked immunospot assay (Elispot) are provided in online supplemental materials and methods section.

RESULTS

Expression of PDL1 is significantly upregulated in the liver of CHB patients and HBV carrier mice

It has been reported that PDL1 can be further upregulated in hepatocytes by HBV infection.[10] Initially, we analysed PDL1 expression in the liver of CHB patients, non-HBV liver disease patients and healthy controls by immunohistochemistry. Consistent with previous studies,[11 27] CHB patients had higher PDL1 expression levels within the liver than non-HBV liver disease patients and healthy controls (online supplemental figure 1A,B). Then, mouse liver cells were collected to evaluate PDL1 expression using flow cytometry. Compared with naïve mice, HBV-infected mice had significantly increased PDL1 expression

on both CD45$^-$ cells and CD45$^+$ cells within the liver (online supplemental figure 1C,D). Taken together, these results indicate that humans and mice with CHB upregulate PDL1 expression in the liver.

We next examined PDL1 expression levels in various tissues of HBV carrier mice. We observed that PDL1 levels on both CD45$^-$ cells and CD45$^+$ cells within the liver were higher than those on corresponding cells within other tissues of HBV carrier mice (figure 1A). To further identify which cell type(s) expresses elevated levels of PDL1, we profiled PDL1 expression levels on different cell types in the liver by flow cytometry. PDL1 expression on DCs was higher than that on other cells in the liver of HBV carrier mice and was significantly higher than that on hepatic DCs from naïve mice (figure 1B, online supplemental figure 1E). These data suggest that HBV infection leads to PDL1 upregulation on DCs within the liver, potentially causing immune tolerance, which could be one of the mechanisms involved in chronic HBV infection. However, anti-PDL1/PD1 treatment as an adjuvant therapy for CHB was not successful, suggesting that blocking PD1/PDL1 signalling alone is not sufficient for reducing the immune tolerance in CHB.[18 28 29]

Anti-PDL1-IFNα heterodimer exerts superior anti-HBV effects through liver targeting

Type I IFNs bind to IFNAR on DCs to increase cross-presentation and directly inhibit HBV replication in infected hepatocytes.[30–32] To overcome PDL1-mediated immune suppression and take advantage of the high PDL1 level in the liver, we generated fusion proteins containing the antigen-binding fragment (Fab) of an anti-PDL1 antibody and IFNα (anti-PDL1-IFNα) in either a homodimeric or heterodimeric format (figure 1C), these proteins could bind to PDL1 and block the PDL1 inhibitory pathway while agonising IFNAR signalling to activate DCs. In addition, control IFNα-Fc and anti-PDL1 proteins were constructed (online supplemental figure 2A). Gel electrophoresis confirmed that the purified fusion proteins were the correct sizes (online supplemental figure 2B,C).

An antiviral biological assay in vitro showed that both homodimeric anti-PDL1-IFNα and heterodimeric anti-PDL1-IFNα effectively inhibited infection and replication by vesicular stomatitis virus expressing green fluorescent protein (VSV-GFP) in PDL1-knockout L929 cells (online supplemental figure 2D). In addition, the results showed that both the homodimer and the heterodimer bound to PDL1 with an affinity similar to that of anti-PDL1 (online supplemental figure 2E, left panel). More importantly, the affinity of anti-PDL1-IFNα for PDL1 was higher than that for IFNAR1 or IFNAR2 for both the homodimer and the heterodimer (online supplemental figure 2E), indicating that anti-PDL1-IFNα may preferentially bind to PDL1^{high} cells over IFNAR$^+$ cells in the liver. Together, these data suggest that both the homodimeric and heterodimeric fusion proteins can bind to PDL1 while maintaining IFNα bioactivity.

Next, we demonstrated that the anti-PDL1-IFNα heterodimer had dose-dependent anti-HBV activity in vivo. Importantly, the results implied that 0.1687 nmol had limited toxicity but exerted strong anti-HBV effects. Neither ALT nor AST was elevated after heterodimer treatment (online supplemental figure 3A,B). Therefore, these data together indicate that the optimal dose of the heterodimer is 0.1687 nmol in vivo, and this dose was used for the remaining experiments in the current study. Subsequently, HBV carrier mice were injected intravenously with fusion proteins on days 1 and 4 (figure 1D). We found that the heterodimer reduced HBsAg and HBeAg levels more significantly than anti-PDL1, IFNα-Fc or the homodimer (figure 1E,F). In addition, the heterodimer significantly reduced HBsAg levels compared with free IFNα (online supplemental figure 3C). The inhibitory effect of the heterodimer on the serum HBV-DNA load was more persistent (figure 1G). Importantly, the heterodimer also significantly reduced the HBsAg and HBeAg levels in the liver (figure 1H). We wondered whether these differences were due to the different liver-targeting abilities of the fusion proteins. Indeed, the concentration in liver tissues was much higher for the heterodimer than for the homodimer or IFNα-Fc (online supplemental figure 3D). Additionally, the serum concentration of the heterodimer was significantly higher within the first few hours after injection (online supplemental figure 3E). Impressively, the heterodimer was approximately 200-fold more potent in inhibiting VSV-GFP infection in L929 cells than in cells not expressing the PDL1 target (PDL1$^{-/-}$ L929 cells), whereas both cell lines showed similar responsiveness to IFNα-Fc (online supplemental figure 4A,B). This result corroborated that the IFNα activity of the heterodimer had the potential to be enhanced through delivery to target cells. Together, these data support the superior anti-HBV effects of the heterodimer in vivo and indicate that the heterodimeric construct is an excellent candidate for the treatment of HBV infection.

Anti-PDL1-IFNα heterodimer achieves synergistic antiviral effects through a positive feedback immune response

We next evaluated whether the anti-PDL1-IFNα heterodimer has the synergistic effect of inhibiting HBV infection and replication. An HBV-infected human hepatocyte assay was performed in the presence of the fusion protein in vitro. The mouse IFNα in the fusion protein was replaced with human IFNα. Interestingly, the levels of HBsAg and HBeAg in the cell culture supernatant were inhibited more significantly by the anti-PDL1-IFNα (human) heterodimer than by the other agents (online supplemental figure 5A,B). Furthermore, we observed that HBV carrier mice treated with a mixture of IFNα-Fc and anti-PDL1 did not show the same inhibitory effect as that achieved with the heterodimer (figure 2A–C). Thus, both the in vitro and in vivo data show that targeted delivery of IFNα by anti-PDL1 is critical for the anti-HBV effect. In addition, we tested whether the anti-HBV effect of the heterodimer is exerted through IFNAR signalling. IFNAR1$^{-/-}$ HBV carrier mice were treated with the heterodimer. The antiviral effect was almost undetectable in the IFNAR1$^{-/-}$ HBV carrier mice, suggesting that the anti-PDL1-IFNα heterodimer plays an anti-HBV role through IFNAR signalling (figure 2D).

We tested the PDL1 level in the liver after anti-PDL1-IFNα heterodimer treatment. Impressively, the heterodimer was able to significantly increase PDL1 expression on both CD45$^-$ cells and CD45$^+$ cells within the liver microenvironment compared with IFNα-Fc (figure 2E,F). Increased PDL1 expression may enhance the liver-specific accumulation of the anti-PDL1-IFNα heterodimer. Collectively, these data suggest that the anti-PDL1-IFNα heterodimer can induce a positive synergistic response, further enhancing liver targeting and better controlling HBV replication.

Anti-PDL1-IFNα heterodimer overcomes immune tolerance by improving DC function

A previous report showed that type I IFNs play a critical role in promoting DC cross-priming to (re)activate T cells.[33] We hypothesised that the anti-PDL1-IFNα heterodimer may preferentially target DCs, which were found to express higher levels

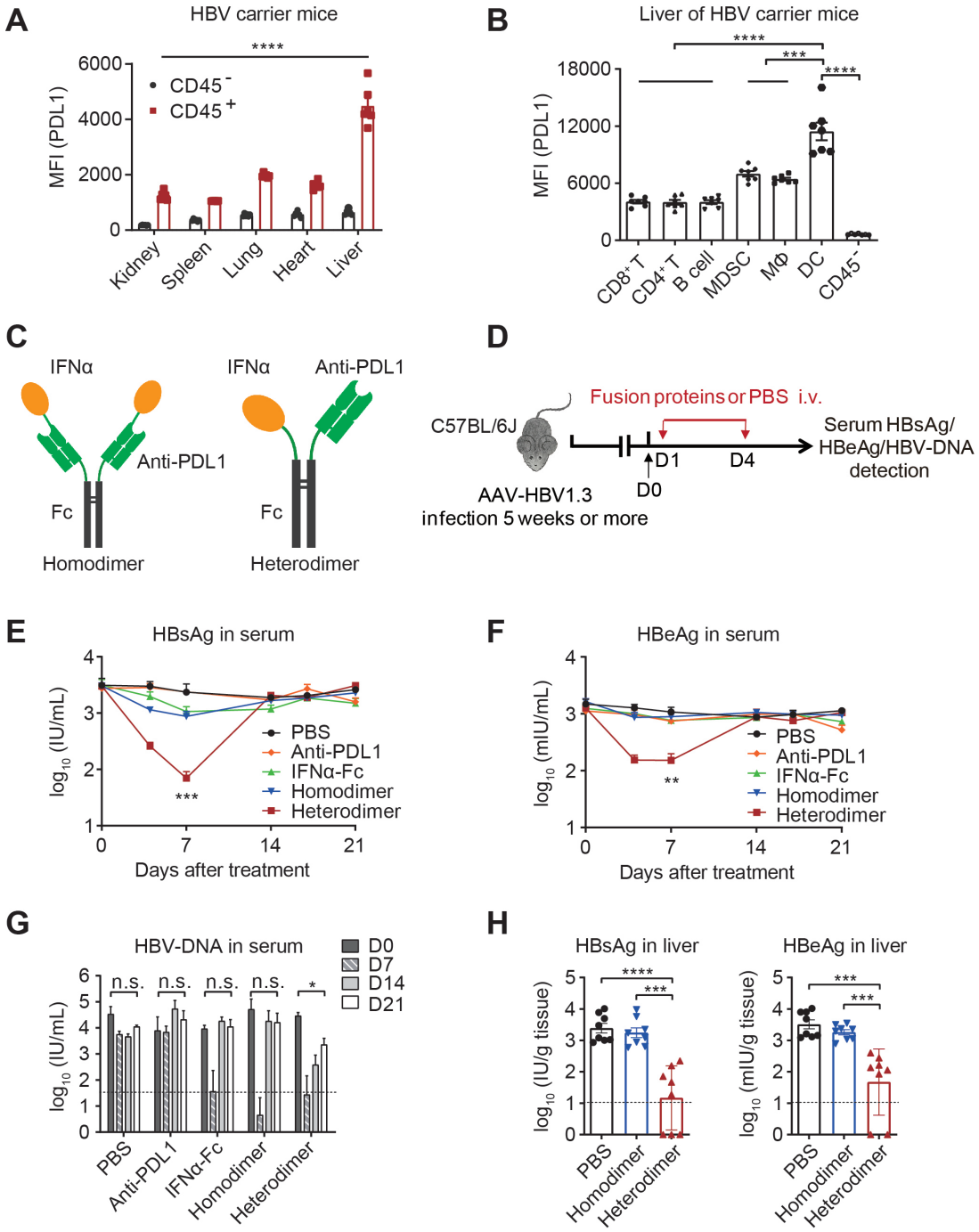

Figure 1 The anti-PDL1-IFNα heterodimer exerts superior anti-HBV effects in vivo. (A) Various tissues of HBV carrier mice were collected (n=6). PDL1 expression levels on $CD45^-$ or $CD45^+$ cells were evaluated by flow cytometry. (B) Liver tissues of HBV carrier mice (n=7) were collected and analysed by flow cytometry. PDL1 expression levels on $CD8^+$ T cells ($CD3^+CD8^+$), $CD4^+$ T cells ($CD3^+CD4^+$), B cells ($B220^+$), MDSCs ($CD11b^+Gr\text{-}1^+$), macrophages ($CD11b^+F4/80^+$), DCs ($CD11c^+MHCII^+$) and $CD45^-$ cells are shown. (C) Schematic structure of the anti-PDL1-IFNα fusion protein in the homodimeric or heterodimeric format. (D) Time schedule for testing the therapeutic effects of fusion proteins in vivo. HBV carrier mice were injected intravenously with fusion proteins two times with a 3-day interval using equimolar amounts of IFNα and anti-PDL1 (0.1687 nmol, as determined by the single subunit). (E–H) HBV carrier mice (n=3–8) were treated with fusion proteins on days 1 and 4 as described in (D). The serum levels of HBsAg (E) and HBeAg (F) were determined using ELISA. The serum levels of HBV-DNA (G) were determined by quantitative real-time PCR. The liver levels of HBsAg and HBeAg (H) on day seven were measured using ELISA. The detection limits in panels G and H are shown as dashed lines. Data are shown as the mean±SEM (A, B and H) or mean+SEM (E–G) and are representative of at least two independent experiments. *p<0.05; **p<0.01; ***p<0.001; ****p<0.0001. DC, dendritic cell; HBeAg, hepatitis B e antigen; HBsAg, hepatitis B surface antigen; HBV, hepatitis B virus; IU, international units; i.v., intravenous; MDSC, myeloid-derived suppressor cell; MFI, mean fluorescence intensity; MΦ, macrophage; n.s., not significant; PBS, phosphate buffer saline; PDL1, programmed death ligand 1.

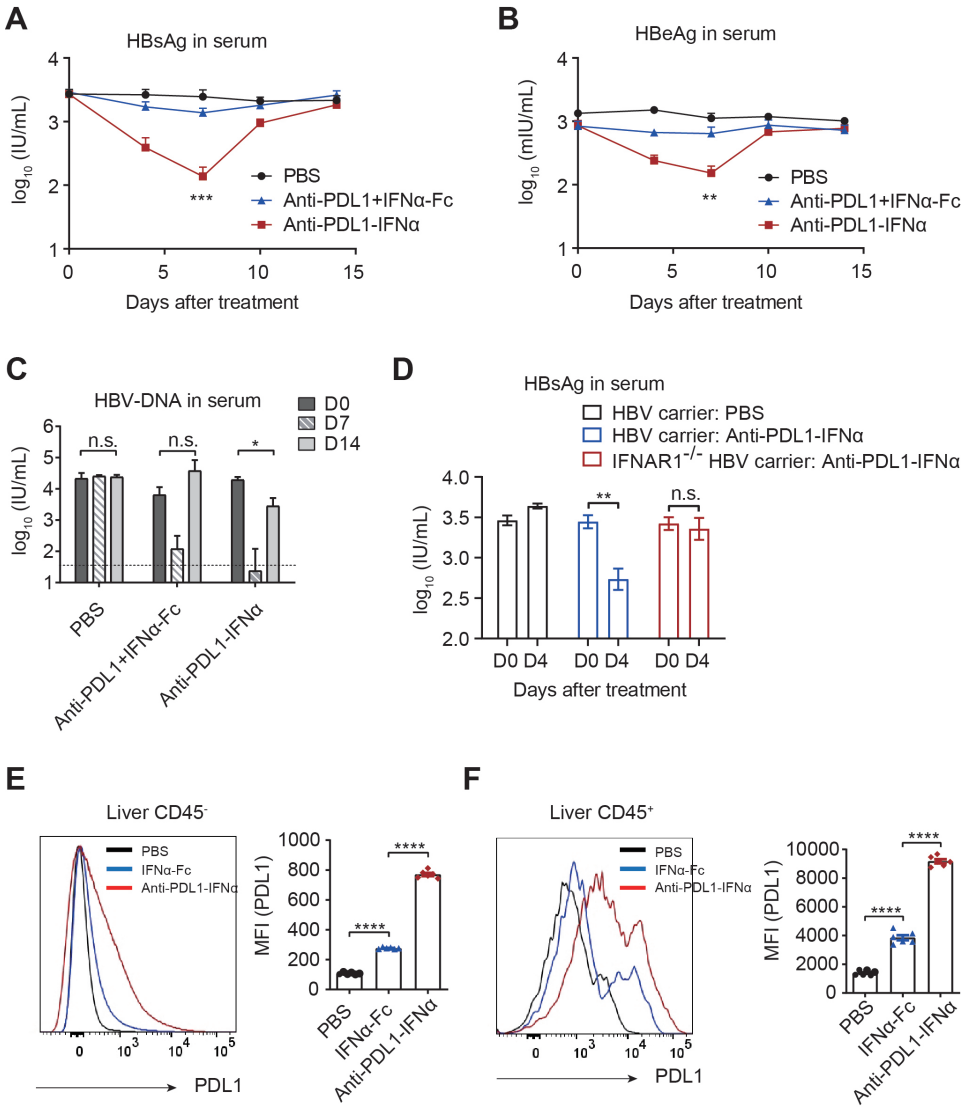

Figure 2 The anti-PDL1-IFNα heterodimer achieves a synergistic antiviral effect via positive synergy of the anti-PDL1 and IFNα signalling axes. (A–C) Serum levels of HBsAg (A), HBeAg (B) and HBV-DNA (C) of HBV carrier mice (n=3–7) that received intravenous injections of fusion proteins (a mixture of anti-PDL1 and IFNα-Fc or only the anti-PDL1-IFNα heterodimer) using equimolar amounts of IFNα and anti-PDL1 (0.1687 nmol, as determined by the single subunit) on days 1 and 4. The detection limit in panel C is shown as a dashed line. (D) HBV carrier mice (n=5) and IFNAR1$^{-/-}$ HBV carrier mice (n=7) were treated with PBS or the anti-PDL1-IFNα heterodimer (0.1687 nmol, 0.8 mg/kg) on day 1. The serum HBsAg levels on day four were detected using ELISA. (E, F) HBV carrier mice (n=6) were injected intravenously with a single dose (equimolar IFNα, as determined by the single subunit) of IFNα-Fc (0.0844 nmol, 0.313 mg/kg) or the anti-PDL1-IFNα heterodimer (0.1687 nmol, 0.8 mg/kg). Three days later, liver tissues were collected, and the PDL1 levels on CD45^{-} (E) and CD45^{+} (F) cells were evaluated by flow cytometry. A representative graph is shown on the left, and the MFI is shown on the right. Data are shown as the mean+SEM (A–C) or mean±SEM (D–F) and are representative of at least two independent experiments. *p<0.05; **p<0.01; ***p<0.001; ****p<0.0001. HBeAg, hepatitis B e antigen; HBsAg, hepatitis B surface antigen; HBV, hepatitis B virus; IU, international units; MFI, mean fluorescence intensity; n.s., not significant; PBS, phosphate buffer saline; PDL1, programmed death ligand 1.

of PDL1 (figure 1B). We thus investigated whether anti-PDL1-IFNα treatment can improve the functions of DCs. HBV carrier mice were treated with a single dose of the anti-PDL1-IFNα heterodimer. Three days later, the DCs in the liver were analysed by flow cytometry (figure 3A). Encouragingly, compared with the other treatments, anti-PDL1-IFNα treatment resulted in significantly increased expression of CD86, CD80 and MHC I on hepatic DCs (figure 3B,C, online supplemental figure 6A,B). These changes are indicative of the development of mature DCs with increased potentials for cross-presentation and costimulation for T cell activation.[34] Impressively, anti-PDL1-IFNα indeed activated the effector function of T cells in HBV carrier mice, as indicated by the significant increases in HBsAg-specific IFN-γ^{+}CD4^{+} and IFN-γ^{+}CD8^{+} T cells in the liver (figure 3D,E, online supplemental figure 6C–F). The role of DCs in anti-PDL1-IFNα treatment was further confirmed in the HBV carrier CD11c-DTR (diphtheria toxin, DTx receptor) mice. DTx treatment significantly reduced DC level. The anti-PDL1-IFNα induced HBsAg-specific T cell and B cell responses were almost abrogated by DTx in the HBV carrier CD11c-DTR mice (online supplemental figure 7A–D). To test whether activated T cells can play an anti-HBV role, CD4- and CD8-depleting antibodies were administered to HBV carrier mice during anti-PDL1-IFNα treatment, which significantly reduced the anti-HBV effect of anti-PDL1-IFNα (figure 3F). A similar result was obtained with Rag1$^{-/-}$ HBV carrier mice

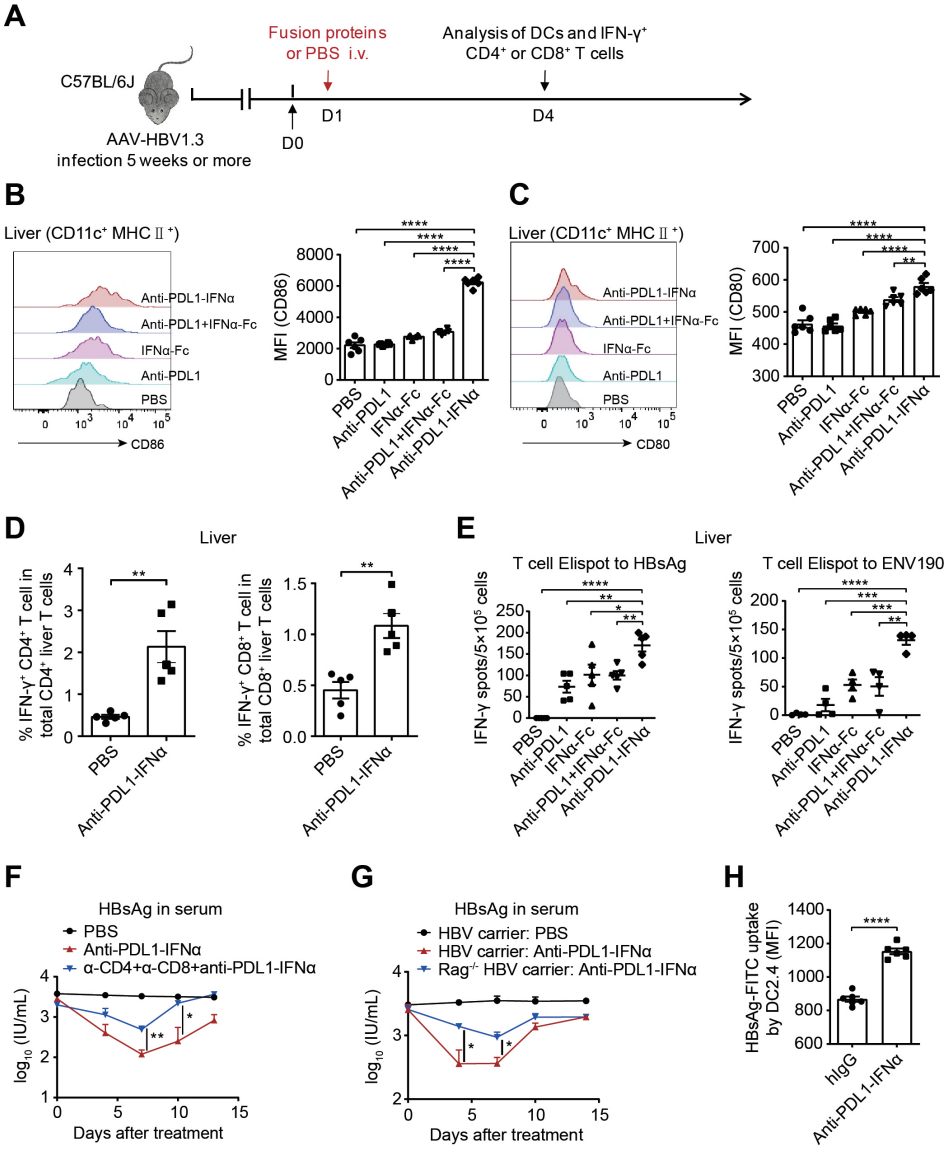

Figure 3 The anti-PDL1-IFNα heterodimer rescues HBsAg-specific T cell immune tolerance by improving DC function. (A) Schematic diagram of a single dose (0.1687 nmol equimolar IFNα and anti-PDL1, as determined by the single subunit) of fusion protein treatment in HBV carrier mice. Three days later, the expression of CD86, CD80 and MHC I on DCs and levels of IFN-γ^+CD4$^+$ and IFN-γ^+CD8$^+$ T cells in the liver were analysed by flow cytometry. (B, C) Hepatic mononuclear cells (n=6) were harvested on day 4. Flow cytometry was performed to analyse the expression of CD86 (B) and CD80 (C) on DCs in the liver. A representative graph is shown on the left, and the MFI is shown on the right. (D, E) Hepatic mononuclear cells (n=4–5) were harvested on day four and stimulated with HBsAg (5 µg/mL; subtype ayw) in the presence of brefeldin A (5 µg/mL) ex vivo. The frequencies of IFN-γ^+ cells among total CD4$^+$ or CD8$^+$ T cells in the liver were examined by flow cytometry (D). Specific T cell responses to HBsAg (subtype ayw) or ENV190 (an HBsAg-specific CD8 peptide) were also tested with a T cell Elispot assay (E). (F) HBV carrier mice (n=3–4) were treated with PBS or the anti-PDL1-IFNα heterodimer (0.1687 nmol, 0.8 mg/kg) on days 1 and 4. For T cell depletion, 200 µg anti-CD4 antibodies and 200 µg anti-CD8 antibodies were injected intraperitoneally into HBV carrier mice twice per week beginning 1 day before anti-PDL1-IFNα heterodimer treatment. The serum HBsAg levels were determined using ELISA. (G) HBV carrier mice (n=5) and Rag1$^{-/-}$ HBV carrier mice (n=5) were treated with PBS or the anti-PDL1-IFNα heterodimer (0.1687 nmol, 0.8 mg/kg) on days 1 and 4. The serum HBsAg levels were determined using ELISA. (H) DC2.4 cells were treated with 1 µg/mL anti-PDL1-IFNα heterodimer and incubated with 1 µg/mL fluorescein isothiocyanate (FITC)-conjugated HBsAg protein for 4 hours. Flow cytometry was performed to analyse the uptake of HBsAg-FTIC. Data are shown as the mean±SEM (B–E and H) or mean+SEM (F, G) and are representative of at least two independent experiments (B, C and E–H) or are pooled from two independent experiments (D). *p<0.05; **p<0.01; ***p<0.001; ****p<0.0001. DC, dendritic cell; HBsAg, hepatitis B surface antigen; HBV, hepatitis B virus; hIgG, human immunoglobulin G; IU, international units; i.v., intravenous; MFI, mean fluorescence intensity; PBS, phosphate buffer saline.

(figure 3G). Collectively, these data support that the activation of T cells by the anti-PDL1-IFNα heterodimer can exert an anti-HBV role, in addition to the direct antiviral effect of the IFNα incorporated in the anti-PDL1-IFNα molecule. To further validate these observations, we tested whether anti-PDL1-IFNα enhances the antigen uptake and processing of DCs. Compared with hIgG treatment, anti-PDL1-IFNα treatment augmented uptake of an HBsAg-FITC protein by DCs in vitro (figure 3H). Taken together, these data indicate that the anti-PDL1-IFNα heterodimer promotes the maturation and antigen-presenting function of DCs, thereby improving the function of HBV-specific T cells.

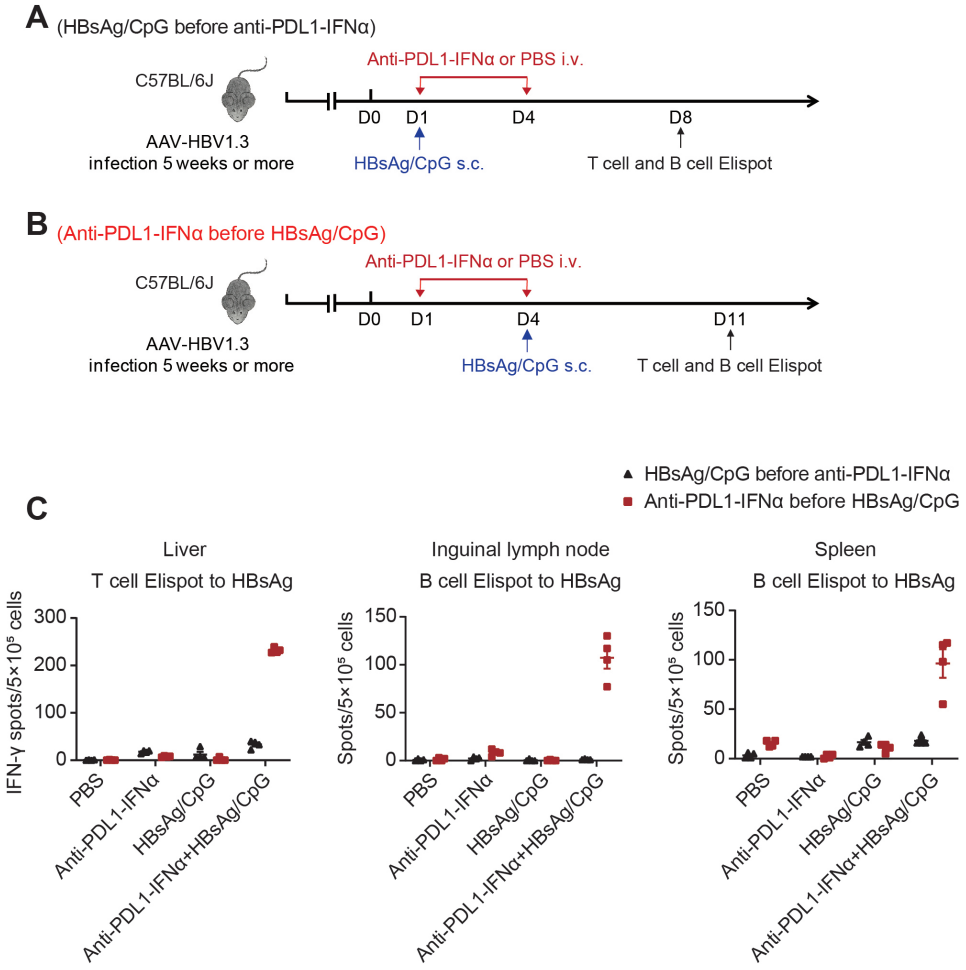

Figure 4 The anti-PDL1-IFNα heterodimer can break tolerance to an HBsAg vaccine. (A) HBV carrier mice (n=4) were immunised subcutaneously with HBsAg/CpG (2 µg/30 µg) on day 1. The anti-PDL1-IFNα heterodimer (0.0422 nmol, 0.2 mg/kg) was injected intravenously on days 1 and 4 (HBsAg/CpG before anti-PDL1-IFNα). One week after immunisation, HBsAg-specific T and B cells were measured by T cell and B cell Elispot assays, respectively. (B) HBV carrier mice (n=4) were injected intravenously with the anti-PDL1-IFNα heterodimer (0.0422 nmol, 0.2 mg/kg) on days 1 and 4. HBsAg/CpG (2 µg/30 µg) was administered subcutaneously on day 4 (anti-PDL1-IFNα before HBsAg/CpG). One week after immunisation, HBsAg-specific T and B cells were measured by T cell and B cell Elispot assays, respectively. (C) A total of 5×10^5 lymphocytes from the liver, inguinal lymph nodes or spleen (n=4) were collected 1 week after immunisation. Specific T cell and B cell responses to HBsAg (subtype ayw) were tested by T cell and B cell Elispot assays, respectively. Data are shown as the mean±SEM and are representative of at least two independent experiments. CpG, cytosine–phosphate–guanine; HBsAg, hepatitis B surface antigen; i.v., intravenous; PBS, phosphate buffer saline; s.c., subcutaneous.

Anti-PDL1-IFNα heterodimer breaks tolerance to an HBsAg vaccine in the chronic HBV mouse model

The above results showed that the anti-PDL1-IFNα heterodimer could inhibit HBV for a period of time and simultaneously improve the cross-presentation and costimulatory the signalling of DCs, suggesting that anti-PDL1-IFNα treatment may provide a 'window' for breaking HBV-induced immune tolerance. We then combined anti-PDL1-IFNα with HBsAg vaccination to test immune responses against this HBV antigen. Impressively, compared with HBsAg vaccination performed before anti-PDL1-IFNα treatment, anti-PDL1-IFNα treatment performed before HBsAg vaccination induced strong HBsAg-specific T and B cell immune responses within the liver, lymph nodes and spleen (figure 4). These results suggest that the anti-PDL1-IFNα heterodimer can break the tolerance to HBsAg to allow effective vaccination in HBV-tolerant mice.

Next, we tested whether this treatment approach can synergize with HBsAg vaccination to treat HBV carrier mice (figure 5A). Notably, the serum HBsAg level dropped significantly in the combination therapy group (anti-PDL1-IFNα combined with HBsAg/CpG vaccination) but not in the monotherapy group (figure 5B). Furthermore, the ayw subtype-specific anti-HBsAg level in the combination therapy group increased significantly for a long time (figure 5C). The serum HBsAg and HBV-DNA levels had dropped to undetectable levels in 7 out of the 10 mice in the combination therapy group on day 129 after the initial treatment. The mice with a reduced serum HBsAg level also showed a significantly higher level of ayw subtype-specific anti-HBsAg antibodies (figure 5D, online supplemental figure 8A–C), suggesting the potential functional cure of CHB in the carrier mice. Importantly, in addition to the reduced HBsAg level in the circulation, intrahepatic HBsAg expression levels were remarkably reduced in the combination therapy group (online supplemental figure 8D). In addition, the HBV-RNA and HBV-DNA loads in the liver measured by real-time PCR were significantly diminished in the combination therapy group (online supplemental figure 9A–C). Overall, the therapeutic strategy of combining anti-PDL1-IFNα administration and HBsAg vaccination could be applied as an effective treatment to achieve a functional cure of CHB.

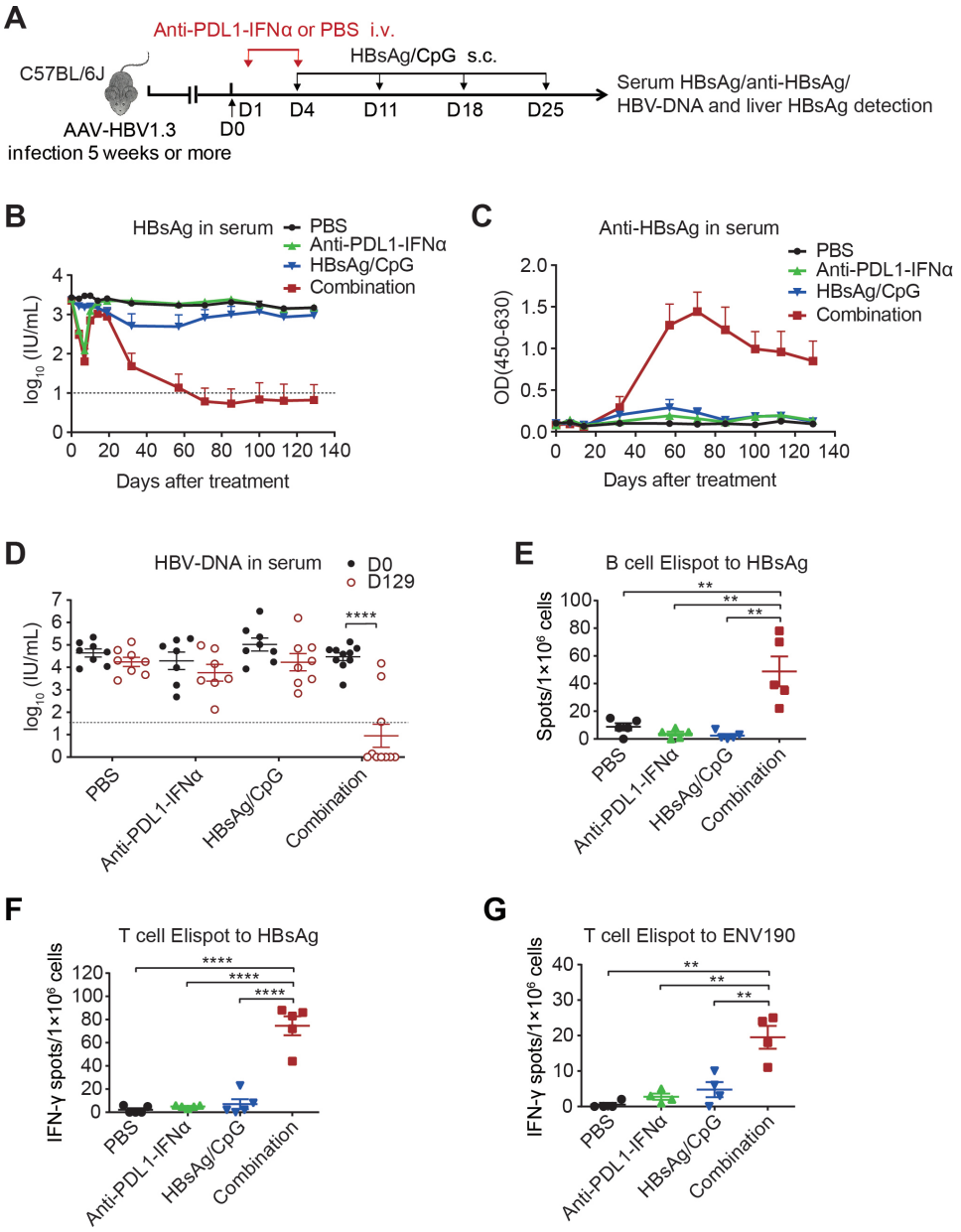

Figure 5 Anti-PDL1-IFNα heterodimer administration combined with HBsAg vaccination produces a functional cure in HBV carrier mice. (A) Time schedule for the anti-PDL1-IFNα heterodimer (0.1687 nmol, 0.8 mg/kg) combined with HBsAg/CpG (2 µg/30 µg) as a vaccine to treat HBV carrier mice. (B, C) The serum HBsAg (B) and ayw subtype-specific anti-HBsAg (C) levels (n=7–10) were monitored by ELISA. (D) Serum HBV-DNA levels (n=7–10) were determined by quantitative real-time PCR. The detection limits in panels B, D are shown as dashed lines. (E–G) A total of 1×10^6 splenocytes from each mouse (n=4–5) were collected on day 129. Specific B cell (E) and T cell (F) responses to HBsAg (subtype ayw) were tested by B cell and T cell Elispot assays, respectively. ENV190-specific $CD8^+$ T cell responses were tested by a T cell Elispot assay (G). Data are shown as the mean+SEM (B, C) or mean±SEM (D–G) and are pooled from two independent experiments. **p<0.01; ****p<0.0001. CpG, cytosine–phosphate–guanine; HBsAg, hepatitis B surface antigen; HBV, hepatitis B virus; IU, international units; i.v., intravenous; OD, optical density; PBS, phosphate buffer saline; s.c., subcutaneous.

HBsAg-specific humoral and cellular immune responses induced by the combination therapy can neutralise HBV and prevent HBV reinfection

We investigated whether the combination therapy can induce immune memory to prevent recurrent HBV infection. The results showed that splenocytes from resolved HBV carrier mice treated with the combination therapy on day 129 produced strong HBsAg-specific B cell responses when stimulated with the HBsAg antigen ex vivo (figure 5E). In addition, splenocytes from resolved HBV carrier mice treated with the combination therapy on day 129 secreted significantly higher levels of IFN-γ when stimulated with the HBsAg antigen or ENV190 (an HBsAg-specific CD8 peptide) ex vivo (figure 5F,G). These data suggest that the resolved HBV carrier mice treated with the combination therapy gained long-term immune memory, which might play an important role in preventing recurrent HBV infection.

To evaluate HBV neutralisation in vivo by assessing antisera from resolved HBV carrier mice treated with the combination therapy, serum samples were collected from resolved HBV carrier mice and injected intravenously into untreated HBV

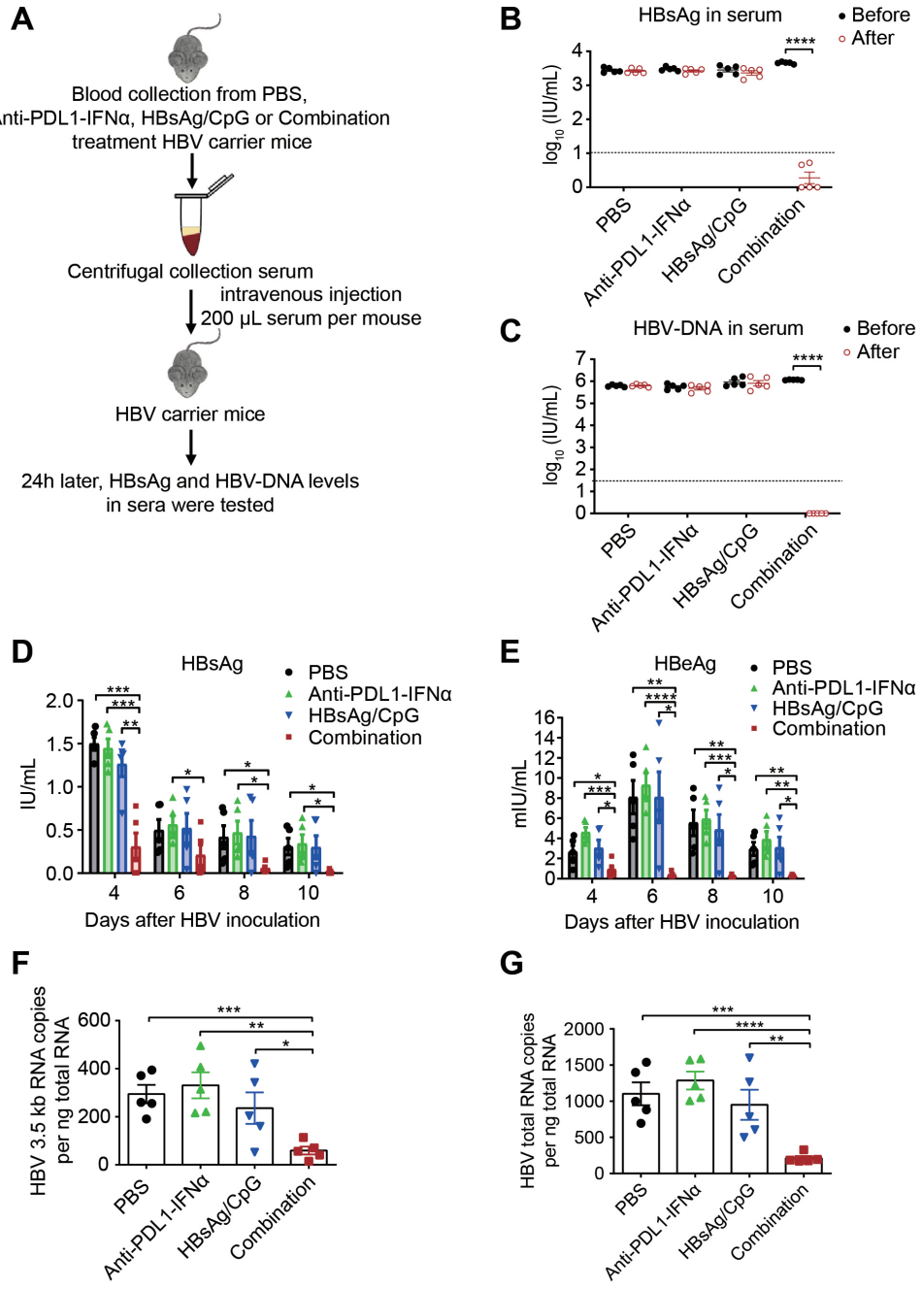

Figure 6 The anti-HBsAg antibodies induced by the combination therapy can neutralise HBV in vivo and prevent HBV from infecting hepatocytes in vitro. (A) Schematic diagram of HBV neutralisation in vivo by using sera collected from PBS-, anti-PDL1-IFNα-, HBsAg/CpG- or combination-treated HBV carrier mice (n=5) on day 71 as described in figure 5A. (B, C) The serum levels of HBsAg (B) and HBV-DNA (C) were assessed via ELISA and quantitative real-time PCR, respectively. The detection limits are shown as dashed lines. (D–G) For studying blocking of HBV infection of hepatocytes in vitro, HepG2-hNTCP cells were incubated with 1×10^7 viral genome equivalents (vg) HBV in the presence of serum collected from PBS-, anti-PDL1-IFNα-, HBsAg/CpG- or combination-treated HBV carrier mice (n=5) on day 129 as described in figure 5A. The levels of HBsAg (D) and HBeAg (E) in the supernatant were detected by ELISA. HepG2-hNTCP cells were collected in TRIzol on day 10, and RNA was extracted. HBV 3.5 kb RNA (F) and HBV total RNA (G) levels were measured by quantitative real-time PCR. Data are shown as the mean±SEM and are representative of at least two independent experiments. *p<0.05; **p<0.01; ***p<0.001; ****p<0.0001. CpG, cytosine–phosphate–guanine; HBeAg, hepatitis B e antigen; HBsAg, hepatitis B surface antigen; HBV, hepatitis B virus; hNTCP, human sodium taurocholate cotransporting polypeptide; IU, international units; PBS, phosphate buffer saline.

carrier mice (figure 6A). The HBsAg and HBV-DNA levels were greatly reduced by the sera from resolved HBV carrier mice treated with the combination therapy, indicating that the anti-sera could effectively eliminate HBV in vivo (figure 6B,C). We next tested the ability of antiserum to prevent HBV infection in vitro. HepG2-hNTCP cells were infected with HBV in the presence of sera from different groups. The levels of HBsAg and HBeAg in the cell culture supernatant were significantly inhibited by the sera from resolved HBV carrier mice treated with combination therapy, in stark contrast to the effects of the sera from the other groups (figure 6D,E). To more accurately detect HBV infection inhibition, HBV replicative intermediates,

including HBV 3.5-kilobase (kb) RNA and HBV total RNA, in HepG2-hNTCP cells were measured, and the results showed a significant reduction in HBV replicative intermediates induced by the sera from resolved HBV carrier mice treated with the combination therapy (figure 6F,G). Taken together, both the in vivo and in vitro results suggest that the combination therapy can induce strong anti-HBsAg immune responses to achieve a functional cure of CHB and prevent HBV reinfection.

DISCUSSION

Breaking HBV-induced immune tolerance, especially inducing a NAb response to HBsAg in CHB patients, has been a difficult goal to reach in the clinic over recent decades.[35] Recently, three well-designed experimental studies in mice showed that clearance of the HBsAg antigen by NAbs or small interfering RNAs followed by active immunisation could induce effective host immune responses against HBV.[23 36 37] However, these strategies for reducing the HBsAg antigen load were passive rather than active ways to improve host immunity, and the NAb strategy was not practical for patients with a high level of HBsAg. In this study, we designed a multifunctional anti-PDL1-IFNα heterodimeric fusion protein that could block the immune checkpoint PDL1, target IFNα to the liver to suppress HBV replication, and promote DC maturation and antigen presentation, providing a 'window' for breaking HBV-induced immune tolerance. Subsequent HBsAg vaccination following anti-PDL1-IFNα treatment could induce a strong anti-HBsAg immune response to achieve a functional cure for CHB.

The PD1/PDL1 pathway plays inhibitory roles in T cell activation and proliferation, leading to immune suppression and PD blockade can enhance T cell function by releasing inhibitory signalling.[38 39] Previous studies and our present data have indicated that PDL1 is highly expressed in the liver of CHB patients[11 27] and chronic HBV carrier mice (online supplemental figure 1), suggesting that an anti-PDL1 antibody could reduce immune suppression on the one hand and function as a liver-targeting antibody on the other hand. In addition, type I IFNs can promote cross-presentation and T cell activation by DCs.[31] However, type I IFNs are one of the most potent inducers of inhibitory PDL1 molecules, which dampen the T cell response.[10 40] The anti-PDL1-IFNα heterodimer not only delivered IFNα specifically to the liver but also blocked PDL1 signalling, turning the contradictory activities into mutually reinforcing activities. Moreover, IFNα upregulated PDL1 expression in the liver, which further enhanced the targeting of anti-PDL1-IFNα to the liver.

PDL1 is substantially upregulated on myeloid DCs (mDCs) from CHB patients and significantly suppresses T cell immune functions. PDL1 blockade enhances mDC-mediated antiviral T cell responses in CHB patients.[41] Activated DCs upregulate the costimulatory molecules CD80, CD86 and CD40 to potently activate $CD4^+$ and $CD8^+$ T cells.[42] Consistently, our findings showed that the anti-PDL1-IFNα heterodimer improved the functions of DCs by upregulating CD86, CD80 and MHC I molecules, which promoted HBsAg antigen uptake, cross-presentation and costimulatory signalling to activate T cells (figure 3). Moreover, increasing antigen-presenting cell function can initiate antigen-specific immune responses rather than nonselectively amplifying preexisting T cell responses.[31] Successful HBV clearance is associated with robust HBV-specific IFN-γ^+CD4^+ and $CD8^+$ T cell responses.[43 44] In this study, we found that improving the functions of DCs could promote the HBsAg vaccination-induced HBsAg-specific antibody response and HBsAg-specific T cell activation, providing important insights for the development of a DC-targeted immunotherapeutic strategy.

In previous studies, an HBsAg-specific lymphoproliferative response and anti-HBsAg production against epitopes contained in the therapeutic vaccine were induced in some CHB patients, but no reductions in serum HBsAg or HBV levels were observed.[45 46] These results suggest that patients may mainly respond to the nonshared epitopes of the recombinant HBsAg vaccine that differ from the epitopes of the subtype of HBV in the infected host but fail to develop anti-HBsAg antibodies specific for most of the shared epitopes, thus failing to clear HBsAg. To avoid misevaluation caused by unmatched epitopes, we infected mice with HBV (genotype D, subtype ayw), immunised them with the same subtype (ayw) of recombinant HBsAg, and measured ayw subtype-specific anti-HBsAg antibodies. Our data showed that only under this experimental condition was a high level of anti-HBsAg antibodies strictly associated with HBsAg clearance, explaining the confusing results of coexisting anti-HBsAg antibodies and HBsAg observed in previously reported experiments and clinical trials.

This study reveals several mechanisms that provide critical information for future CHB therapy. First, anti-PDL1-IFNα therapy was a rather short-term treatment that was effective for targeting IFNα to $PDL1^+$ intrahepatic cells and less toxic than prolonged high-dose treatment with IFNs. Second, anti-PDL1-IFNα could deliver immunomodulatory molecules that reduced PDL1-mediated resistance through both checkpoint blockade and enhancement of DC function. Thus, anti-PDL1-IFNα treatment could break HBV-induced immune tolerance by revitalising innate and adaptive immune cells to promote HBsAg vaccine-induced HBsAg-specific T cell and B cell responses. Third, anti-PDL1-IFNα created a positive synergistic response between checkpoint blockade and IFNα signalling and might further enhance the targeting effect through IFNα-induced PDL1 upregulation. Finally, anti-PDL1-IFNα therapy combined with HBsAg vaccine administration could induce a high-level, persistent anti-HBsAg response for efficient viral clearance and protective immunity in a chronic HBV mouse model, offering a promising translatable combination therapeutic strategy for achieving a functional cure of CHB.

Author affiliations
[1]Key Laboratory of Infection and Immunity, Institute of Biophysics, Chinese Academy of Sciences, Beijing, China
[2]Department of Basic Medical Sciences, School of Medicine, Tsinghua University, Beijing, China
[3]Senior Department of Infectious Diseases, 5th Medical Center of Chinese PLA General Hospital, Beijing, China
[4]Senior Department of Liver Disease, 5th Medical Center of Chinese PLA General Hospital, Beijing, China

Acknowledgements We thank Dr. Wenhui Li for providing the HepG2-hNTCP cell line and HBV virus (ayw subtype) for HBV infection experiment in vitro. We thank Dr. Haidong Tang for generously providing $IFNAR1^{-/-}$ mice. We thank the faculty in the animal facility and technical platform for mouse breeding and technical assistance in IBP.

Contributors HP is responsible for the overall content as the guarantor. C-YM, HP and Y-XF conceived and designed the experiments; HP and Y-XF supervised the project; C-YM performed the experiments, analyzed the data; C-YM, HP and Y-XF wrote the manuscript. SS, YL and HX performed or contributed to specific experiments. CZ, MZ and F-SW provided human liver tissue samples and expert advices.

Funding This work is funded by the National Key R&D Program of China (2018ZX10301-404) to HP.

Competing interests None declared.

Patient consent for publication Not applicable.

Ethics approval The study was approved by the ethics committee of the Fifth Medical Center of Chinese PLA General Hospital (No. 2018006D), and written informed consent was obtained from each subject or their guardian. Participants gave informed consent to participate in the study before taking part.

Provenance and peer review Not commissioned; externally peer reviewed.

Data availability statement All data relevant to the study are included in the article or uploaded as online supplemental information.

ORCID iDs
Chao Zhang http://orcid.org/0000-0001-8126-8145
Fu-Sheng Wang http://orcid.org/0000-0002-8043-6685
Hua Peng http://orcid.org/0000-0002-2482-5475

REFERENCES

1 Word Health Organisation. *Global hepatitis report 2017*. Geneva: World Health Organisation, 2017.
2 Trépo C, Chan HLY, Lok A. Hepatitis B virus infection. *Lancet* 2014;384:2053–63.
3 Terrault NA, Bzowej NH, Chang K-M, *et al*. AASLD guidelines for treatment of chronic hepatitis B. *Hepatology* 2016;63:261–83.
4 , European Association for the Study of the Liver. Electronic address: easloffice@easloffice.eu, European Association for the Study of the Liver. EASL 2017 clinical practice guidelines on the management of hepatitis B virus infection. *J Hepatol* 2017;67:370–98.
5 Sarin SK, Kumar M, Lau GK, *et al*. Asian-Pacific clinical practice guidelines on the management of hepatitis B: a 2015 update. *Hepatol Int* 2016;10:1–98.
6 Kim G-A, Lim Y-S, An J, *et al*. HBsAg seroclearance after nucleoside analogue therapy in patients with chronic hepatitis B: clinical outcomes and durability. *Gut* 2014;63:1325–32.
7 Scaglione SJ, Lok ASF. Effectiveness of hepatitis B treatment in clinical practice. *Gastroenterology* 2012;142:1360–8.
8 Lok ASF, McMahon BJ, Brown RS, *et al*. Antiviral therapy for chronic hepatitis B viral infection in adults: a systematic review and meta-analysis. *Hepatology* 2016;63:284–306.
9 Liu L, Hou J, Xu Y, *et al*. PD-L1 upregulation by IFN-α/γ-mediated STAT1 suppresses anti-HBV T cell response. *PLoS One* 2020;15:e0228302.
10 Mühlbauer M, Fleck M, Schütz C, *et al*. PD-L1 is induced in hepatocytes by viral infection and by interferon-alpha and -gamma and mediates T cell apoptosis. *J Hepatol* 2006;45:520–8.
11 Chen J, Wang X-M, Wu X-J, *et al*. Intrahepatic levels of PD-1/PD-L correlate with liver inflammation in chronic hepatitis B. *Inflamm Res* 2011;60:47–53.
12 Thomson AW, Knolle PA. Antigen-Presenting cell function in the tolerogenic liver environment. *Nat Rev Immunol* 2010;10:753–66.
13 Peng Q, Qiu X, Zhang Z, *et al*. PD-L1 on dendritic cells attenuates T cell activation and regulates response to immune checkpoint blockade. *Nat Commun* 2020;11:4835.
14 Topalian SL, Hodi FS, Brahmer JR, *et al*. Safety, activity, and immune correlates of anti-PD-1 antibody in cancer. *N Engl J Med* 2012;366:2443–54.
15 Brahmer JR, Tykodi SS, Chow LQM, *et al*. Safety and activity of anti-PD-L1 antibody in patients with advanced cancer. *N Engl J Med* 2012;366:2455–65.
16 Salimzadeh L, Le Bert N, Dutertre C-A, *et al*. PD-1 blockade partially recovers dysfunctional virus-specific B cells in chronic hepatitis B infection. *J Clin Invest* 2018;128:4573–87.
17 Jacobi FJ, Wild K, Smits M, *et al*. OX40 stimulation and PD-L1 blockade synergistically augment HBV-specific CD4 T cells in patients with HBeAg-negative infection. *J Hepatol* 2019;70:1103–13.
18 Gane E, Verdon DJ, Brooks AE, *et al*. Anti-PD-1 blockade with nivolumab with and without therapeutic vaccination for virally suppressed chronic hepatitis B: a pilot study. *J Hepatol* 2019;71:900–7.
19 Op den Brouw ML, Binda RS, van Roosmalen MH, *et al*. Hepatitis B virus surface antigen impairs myeloid dendritic cell function: a possible immune escape mechanism of hepatitis B virus. *Immunology* 2009;126:280–9.
20 Li F, Wei H, Wei H, *et al*. Blocking the natural killer cell inhibitory receptor NKG2A increases activity of human natural killer cells and clears hepatitis B virus infection in mice. *Gastroenterology* 2013;144:392–401.
21 Wang X, Dong Q, Li Q, *et al*. Dysregulated response of follicular helper T cells to hepatitis B surface antigen promotes HBV persistence in mice and associates with outcomes of patients. *Gastroenterology* 2018;154:2222–36.
22 Gehring AJ, Ann D'Angelo J. Dissecting the dendritic cell controversy in chronic hepatitis B virus infection. *Cell Mol Immunol* 2015;12:283–91.
23 Zhu D, Liu L, Yang D, *et al*. Clearing persistent extracellular antigen of hepatitis B virus: an immunomodulatory strategy to reverse tolerance for an effective therapeutic vaccination. *J Immunol* 2016;196:3079–87.
24 Bian Y, Zhang Z, Sun Z, *et al*. Vaccines targeting preS1 domain overcome immune tolerance in hepatitis B virus carrier mice. *Hepatology* 2017;66:1067–82.
25 Dion S, Bourgine M, Godon O, *et al*. Adeno-Associated virus-mediated gene transfer leads to persistent hepatitis B virus replication in mice expressing HLA-A2 and HLA-DR1 molecules. *J Virol* 2013;87:5554–63.
26 Wang W, Zhou X, Bian Y, *et al*. Dual-targeting nanoparticle vaccine elicits a therapeutic antibody response against chronic hepatitis B. *Nat Nanotechnol* 2020;15:406–16.
27 Wenjin Z, Chuanhui P, Yunle W, *et al*. Longitudinal fluctuations in PD1 and PD-L1 expression in association with changes in anti-viral immune response in chronic hepatitis B. *BMC Gastroenterol* 2012;12:109.
28 El-Khoueiry AB, Sangro B, Yau T, *et al*. Nivolumab in patients with advanced hepatocellular carcinoma (CheckMate 040): an open-label, non-comparative, phase 1/2 dose escalation and expansion trial. *Lancet* 2017;389:2492–502.
29 Zhang X, Zhou Y, Chen C, *et al*. Hepatitis B virus reactivation in cancer patients with positive hepatitis B surface antigen undergoing PD-1 inhibition. *J Immunother Cancer* 2019;7:322.
30 Sadler AJ, Williams BRG. Interferon-Inducible antiviral effectors. *Nat Rev Immunol* 2008;8:559–68.
31 Yang X, Zhang X, Fu ML, *et al*. Targeting the tumor microenvironment with interferon-β bridges innate and adaptive immune responses. *Cancer Cell* 2014;25:37–48.
32 Wang Y-X, Niklasch M, Liu T, *et al*. Interferon-Inducible MX2 is a host restriction factor of hepatitis B virus replication. *J Hepatol* 2020;72:865–76.
33 Deng L, Liang H, Xu M, *et al*. STING-dependent cytosolic DNA sensing promotes radiation-induced type I interferon-dependent antitumor immunity in immunogenic tumors. *Immunity* 2014;41:843–52.
34 Raeber ME, Rosalia RA, Schmid D, *et al*. Interleukin-2 signals converge in a lymphoid-dendritic cell pathway that promotes anticancer immunity. *Sci Transl Med* 2020;12:eaba5464.
35 Bertoletti A, Gehring A. Therapeutic vaccination and novel strategies to treat chronic HBV infection. *Expert Rev Gastroenterol Hepatol* 2009;3:561–9.
36 Shi B, Wu Y, Wang C, *et al*. Evaluation of antiviral - passive - active immunization ("sandwich") therapeutic strategy for functional cure of chronic hepatitis B in mice. *EBioMedicine* 2019;49:247–57.
37 Michler T, Kosinska AD, Festag J, *et al*. Knockdown of virus antigen expression increases therapeutic vaccine efficacy in high-titer hepatitis B virus carrier mice. *Gastroenterology* 2020;158:1762–75.
38 Nurieva R, Thomas S, Nguyen T, *et al*. T-cell tolerance or function is determined by combinatorial costimulatory signals. *Embo J* 2006;25:2623–33.
39 Chen L. Co-inhibitory molecules of the B7-CD28 family in the control of T-cell immunity. *Nat Rev Immunol* 2004;4:336–47.
40 Liang Y, Tang H, Guo J, *et al*. Targeting IFNα to tumor by anti-PD-L1 creates feedforward antitumor responses to overcome checkpoint blockade resistance. *Nat Commun* 2018;9:4586.
41 Chen L, Zhang Z, Chen W, *et al*. B7-H1 up-regulation on myeloid dendritic cells significantly suppresses T cell immune function in patients with chronic hepatitis B. *J Immunol* 2007;178:6634–41.
42 Cella M, Facchetti F, Lanzavecchia A, *et al*. Plasmacytoid dendritic cells activated by influenza virus and CD40L drive a potent Th1 polarization. *Nat Immunol* 2000;1:305–10.
43 Wang H, Luo H, Wan X, *et al*. TNF-α/IFN-γ profile of HBV-specific CD4 T cells is associated with liver damage and viral clearance in chronic HBV infection. *J Hepatol* 2020;72:45–56.
44 Thimme R, Wieland S, Steiger C, *et al*. CD8(+) T cells mediate viral clearance and disease pathogenesis during acute hepatitis B virus infection. *J Virol* 2003;77:68–76.
45 Vandepapelière P, Lau GKK, Leroux-Roels G, *et al*. Therapeutic vaccination of chronic hepatitis B patients with virus suppression by antiviral therapy: a randomized, controlled study of co-administration of HBsAg/AS02 candidate vaccine and lamivudine. *Vaccine* 2007;25:8585–97.
46 Xu D-Z, Wang X-Y, Shen X-L, *et al*. Results of a phase III clinical trial with an HBsAg-HBIG immunogenic complex therapeutic vaccine for chronic hepatitis B patients: experiences and findings. *J Hepatol* 2013;59:450–6.

Engineered anti-PDL1 with IFNα targets both immunoinhibitory and activating signals in the liver to break HBV immune tolerance

Chao-Yang Meng,[1] Shiyu Sun,[1] Yong Liang,[2] Hairong Xu,[1] Chao Zhang,[3] Min Zhang,[4] Fu-Sheng Wang,[3] Yang-Xin Fu,[2,*] Hua Peng[1,*]

[1]Key Laboratory of Infection and Immunity, Institute of Biophysics, Chinese Academy of Sciences, Beijing, China;

[2]Department of Basic Medical Sciences, School of Medicine, Tsinghua University, Beijing, China;

[3]Senior Department of Infectious Diseases, the Fifth Medical Center of Chinese PLA General Hospital, National Clinical Research Center for Infectious Diseases, Beijing, China;

[4]Senior Department of Liver Disease, the Fifth Medical Center of Chinese PLA General Hospital, Beijing, China

[*]Corresponding author. Email: yangxinfu@tsinghua.edu.cn; hpeng@ibp.ac.cn

Supplementary Materials and Methods

Cloning, expression, and purification of anti-PDL1-IFNα fusion proteins

Production of anti-PDL1-IFNα fusion proteins has been previously described with some modifications.[40] Briefly, the variable regions of the light-chain and heavy-chain of the anti-PDL1 antibody (YW243.55.S70) sequence were synthesized according to a patent (Patent No.: US8217149 B2). Human IgG1 Fc was inserted into the C-terminal of the heavy chain. The entire sequence was cloned into the pEE12.4 vector (Lonza). Murine IFNα4 or human IFNα2 cDNA sequence was cloned and inserted into the N-terminal of human IgG1 Fc. Murine IFNα4 or human IFNα2 with Fc was cloned into the pEE6.4 vector (Lonza). Heterodimer of anti-PDL1 and murine IFNα4 or human IFNα2 was achieved by using the knobs-into-holes technique. Murine IFNα4 or human IFNα2 was fused to the "Holes" (T366S, L368A, Y407V) arm, and anti-PDL1 heavy-chain was fused to the "Knobs" (T366W) arm (Fc CH2 CH3). The murine IFNα4 or human IFNα2-holes, anti-PDL1 heavy-chain-knobs and anti-PDL1 light-chain plasmids were transiently transfected into 293F cells at a ratio of 2:1:2. For homodimer of anti-PDL1 and IFNα4, murine IFNα4 cDNA sequence was inserted into the N-terminal of anti-PDL1 heavy-chain by a GGGGSGGGGSGGGGSGGGGS linker. The IFNα4-anti-PDL1 heavy-chain and light-chain plasmids were transiently transfected into 293F cells at a ratio of 1:1. Supernatants were collected on day 7 after transfection. The fusion proteins were purified using a Protein A-Sepharose column according to the manufacturer's protocol (Repligen Corporation, USA).

Enzyme-linked immunosorbent assay (ELISA)

ELISA kits for HBsAg and HBeAg testing were purchased from Shanghai Kehua Bio-engineering Co., Ltd. (Shanghai, China). HBsAg and HBeAg were measured according to the manufacturer's instructions. The peptides for ayw subtype-specific anti-HBsAg testing 111-140 amino acids (PGSSTTSTGPCRTCMTTAQGTSMYPSCCCT; subtype ayw) with the same encoding sequence in AAV-HBV1.3 were synthesized by China Peptides Co., Ltd. (Shanghai, China). The region from 111 to 140 amino acids is the immunodominant region of HBsAg shared by all serotypes and genotypes of HBV. For ELISA to test ayw subtype-specific anti-HBsAg in sera, plates were coated with 111-140 amino acids at 5 μg/mL in phosphate-buffered saline (PBS) at 4°C overnight. After blocking with blocking buffer (PBS containing 5% fetal bovine serum, FBS), samples were added at 1:100 dilution. Then, horseradish peroxidase (HRP)-conjugated goat anti-mouse IgG (CWbio, Beijing, China) was used for chromogenic reaction. The absorbance at 450-630 nm was detected using a microplate reader (Molecular Devices, USA). Homogenate extracts from mice liver tissues were used to determine the levels of HBsAg and HBeAg in the liver by ELISA. The affinities of anti-PDL1-IFNα (heterodimer or homodimer) to PDL1 (produced in house) or IFNAR (IFNAR1 was purchased from Sino Biological, Beijing, China; IFNAR2 was purchased from Biorbyt, Cambridge, UK) binding were measured using ELISA. EC_{50} was calculated by non-linear regression of the dose–response curves using Prism software (GraphPad Software). For ELISA to detect human Fc, plates were coated with 5 μg/mL goat anti-human IgG, and goat anti-human IgG-HRP (CWbio, Beijing, China) was used as detection antibody.

Antiviral activity of anti-PDL1-IFNα

The PDL1$^{-/-}$ or not L929 fibroblast cell line sensitive to vesicular stomatitis virus (VSV) infection was used to quantify the biological activity of IFNα. Cells were incubated with serial dilutions of anti-PDL1-IFNα (heterodimer or homodimer) or IFNα-Fc (equimolar IFNα, as determined by the single subunit) at 37 °C overnight. The next day, the cells were infected with VSV-GFP (green fluorescent protein) at multiplicity of infection (MOI) = 5 and cultured for another 16 hours. Then, the cells were collected and fixed with 4% paraformaldehyde (PFA). Data were acquired and analyzed using a FACS Calibur or LSRFortessa flow cytometer (BD Biosciences, USA) and FlowJo software (TreeStar), respectively. GFP$^+$ cells were defined as virus-infected cells. The MFI of GFP$^+$ was defined as virus replication intensity. IC_{50} was calculated by non-linear regression of the dose–response curves using Prism software (GraphPad Software).

Tissue distribution and serum concentration of anti-PDL1-IFNα

HBV carrier mice were injected intravenously with a single dose (equimolar) 0.1687 nmol IFNα-Fc (0.625 mg/kg), homodimer (1.264 mg/kg) or heterodimer (0.8 mg/kg) fusion protein. Mice sera were collected, and tissues were harvested after perfusion at the indicated time points. The levels of human Fc in sera or homogenate extracts from different tissues were measured by ELISA.

HBV DNA and RNA detection

Serum HBV-DNA was measured following the manufacturer's instructions (Sansure Biotech, Changsha, China). The lower limit of HBV-DNA detection was 30 IU/mL. Liver HBV DNA was extracted using a gDNA kit (Tiagen Biotech, Beijing, China). Liver total RNA was extracted using TRIzol reagent (Invitrogen, USA). RNA was reverse transcribed into cDNA using the RevertAid First Strand cDNA synthesis Kit (Thermo Scientific, USA). Real-time PCR was performed using SYBR Premix Ex Taq kit (Takara, Japan) on an ABI QuantStudio 7 Flex real-time PCR system instrument (Applied Biosystems, USA). For liver HBV DNA detection, the primers are used as forward, 5′-CACATCAGGATTCCTAGGACC-3′; reverse, 5′-GGTGAGTGATTGGAGGTTG-3′. For liver HBV RNA detection, the primers are used as follows: HBV 3.5-kb RNA (forward, 5′-GAGTGTGGATTCGCACTCC-3′; reverse, 5′-GAGGCGAGGGAGTTCTTCT-3′) and HBV total RNA (forward, 5′-TCACCAGCACCATGCAAC-3′; reverse, 5′-AAGCCACCCAAGGCACAG-3′). For β-actin detection, the primers are used as forward, 5′-CTGACGGCCAGGTCATCACTA-3′; reverse, 5′-CCGGACTCATCGTACTCCTGC-3′. The $2^{-\Delta\Delta Ct}$ method was used to calculate relative target gene expression to β-actin.

Inhibition HBV infection assay in vitro

The HepG2-hNTCP cell line and HBV (genotype D, subtype ayw) virus were kindly provided by Professor Wenhui Li (National Institute of Biological Sciences, Beijing, China). In vitro HBV infection and inhibition assays were performed as previously reported.[24] Briefly, 1×10^7 copies of genome-equivalent HBV were inoculated into the culture medium of 1×10^5 HepG2-hNTCP cells in 48-well plates in the presence of sera from HBV carrier

mice with different treatments and incubated for 24 hours at 37 °C. Then, the cells were washed with medium three times and maintained in primary hepatocytes maintenance medium (PMM) (William's E medium [Gibco, USA] with 3 μg/mL insulin, 5 μg/mL transferrin, 5 ng/mL sodium selenite [insulin–transferrin–sodium selenite; Corning, USA], 2 mM L-glutamine, 10 ng/mL epidermal growth factor [Sigma-Aldrich, USA], 2% dimethyl sulfoxide, 100 U/mL penicillin and 100 μg/mL streptomycin). The medium was changed every 2 days. HBV infection at different time points was analyzed by measuring HBsAg and HBeAg in culture medium supernatant and detecting HBV RNAs in HepG2-hNTCP cells.

For the fusion protein inhibits HBV infection in vitro, HepG2-hNTCP cells in 48-well plates (1×10^5 cells/well) were incubated with serial dilutions of anti-PDL1-IFNα (human) heterodimer, IFNα-Fc (human), or the mixture of IFNα-Fc (human) and anti-PDL1 (equimolar IFNα and anti-PDL1, as determined by the single subunit) at 37 °C overnight. The next day, the cells were infected with 1×10^7 copies of genome-equivalent HBV and cultured for another 24 hours. Then, the cells were washed with medium three times and maintained in PMM. Three days later, the culture supernatants were collected. Levels of HBsAg and HBeAg in the supernatant were measured by ELISA.

Immunohistochemistry

Paraffin-embedded human liver tissue sections at 5 μm were used for PDL1 detection with rabbit anti-PDL1 polyclonal antibody (abs136046, Absin Bioscience Inc., China) and HRP-labeled goat anti-rabbit secondary antibody (PV-6001, Zhongshan Jinqiao

Biotechnology Co., Ltd., China). Then, slides were incubated with 3,3-diaminobenzidine tetrahydrochloride (DAB) chromogen solution (ZLI-9018, Zhongshan Jinqiao Biotechnology Co., Ltd., China), and counterstained with hematoxylin (G1080, Beijing Solarbio Science & Technology Co., Ltd., China). Images were acquired using a Nikon-EclipseTi microscope and NIS software (Nikon, Japan).

Construction of HBV carrier CD11c-DTR mice

C57BL/6J mice (8 weeks old) were irradiated with a 60Co Gammacell source at 10 Gy (1Gy/min). 5×10^6 bone marrow cells from donor mice (CD11c-DTR mice) were intravenously transferred to each mouse 24 hours after irradiation. The chimaeras were given prophylactic water containing antibiotics for 4 weeks following irradiation. Six weeks after bone marrow transplantation, the mice were injected with the AAV-HBV1.3 virus through the tail vein (1×10^{11} viral genome copies per mouse). Five weeks after virus infection, the stable HBV carrier CD11c-DTR mice (serum HBsAg > 1000 IU/mL) were selected for immune therapy study.

Single-cell suspension and flow cytometry analysis

An enzymatic digestion method was utilized to isolate hepatic mononuclear cells.[24] Briefly, mice liver tissues were digested with collagenase IV (1 mg/mL; Roche) and DNase I (100 μg/mL; Roche). Then, the cells were further purified with 40% and 70% Percoll solutions (GE Healthcare) by centrifugation. The hepatic mononuclear cells were collected from the interface, and the erythrocytes were lysed with ammonium-chloride-potassium (ACK)

buffer. Splenocytes were collected, and the erythrocytes were lysed with ACK buffer. Inguinal lymph nodes were digested with collagenase IV (1 mg/mL; Roche) and DNase I (100 μg/mL; Roche), then the cells were collected.

For flow cytometric analysis, single cells were suspended in FACS buffer, blocked with anti-CD16/32 (clone 2.4G2), and incubated with fluorescently labelled antibodies. For intracellular IFN-γ staining, cells were stimulated with 5 μg/mL HBsAg (subtype ayw) ex vivo at 37°C for 18 hours. Brefeldin A (5 μg/mL; BioLegend) was added in the last 6 hours. Then, the cells were harvested and FACS staining was performed. Antibodies used for flow cytometry analysis had been listed in Supplementary Table 2. DAPI or LIVE/DEAD™ fixable yellow dye (Invitrogen) was used to exclude dead cells. To quantitate the intracellular uptake of HBsAg antigen, DC2.4 cells were incubated with 1 μg/mL anti-PDL1-IFNα heterodimer and 1 μg/mL FITC-conjugated HBsAg at 37°C for 4 hours. Data were acquired and analyzed using an LSRFortessa flow cytometer (BD Biosciences, USA) and FlowJo software (TreeStar), respectively.

Enzyme-linked immunospot assay (Elispot)

For B cell Elispot assay, 10 μg/mL HBsAg (subtype ayw, 50 μL/well) was coated onto 96-well Elispot plates (BD Biosciences, USA) at 4 °C overnight. After blocking with RPMI 1640 medium containing 10% FBS, splenocytes or inguinal lymph node cells in 100 μL complete RPMI 1640 medium were added to the wells. After 6 hours incubation at 37 °C, HBsAg-specific IgG was analyzed using biotinylated donkey anti-mouse IgG (CWbio, Beijing, China) and streptavidin-HRP (BD Biosciences, USA). Specific T cell responses

were tested by IFN-γ Elispot assay. Hepatic mononuclear cells or splenocytes were incubated for 48 hours at 37 °C in complete RPMI 1640 medium containing 5 μg/mL HBsAg (subtype ayw) or 10 μg/mL ENV190-197 peptides (VWLSVIWM; an HBsAg-specific CD8 peptide) in an IFN-γ Elispot plate (BD Biosciences, USA). After incubation, the IFN-γ secretion was analyzed using biotinylated anti-mouse IFN-γ antibody and streptavidin-HRP (BD Biosciences, USA). The spots were visualized with 3-amino-9-ethylcarbazole (AEC) substrate (BD Biosciences, USA) and were quantified with the ImmunoSpot Analyzer (Cellular Technology Ltd., USA).

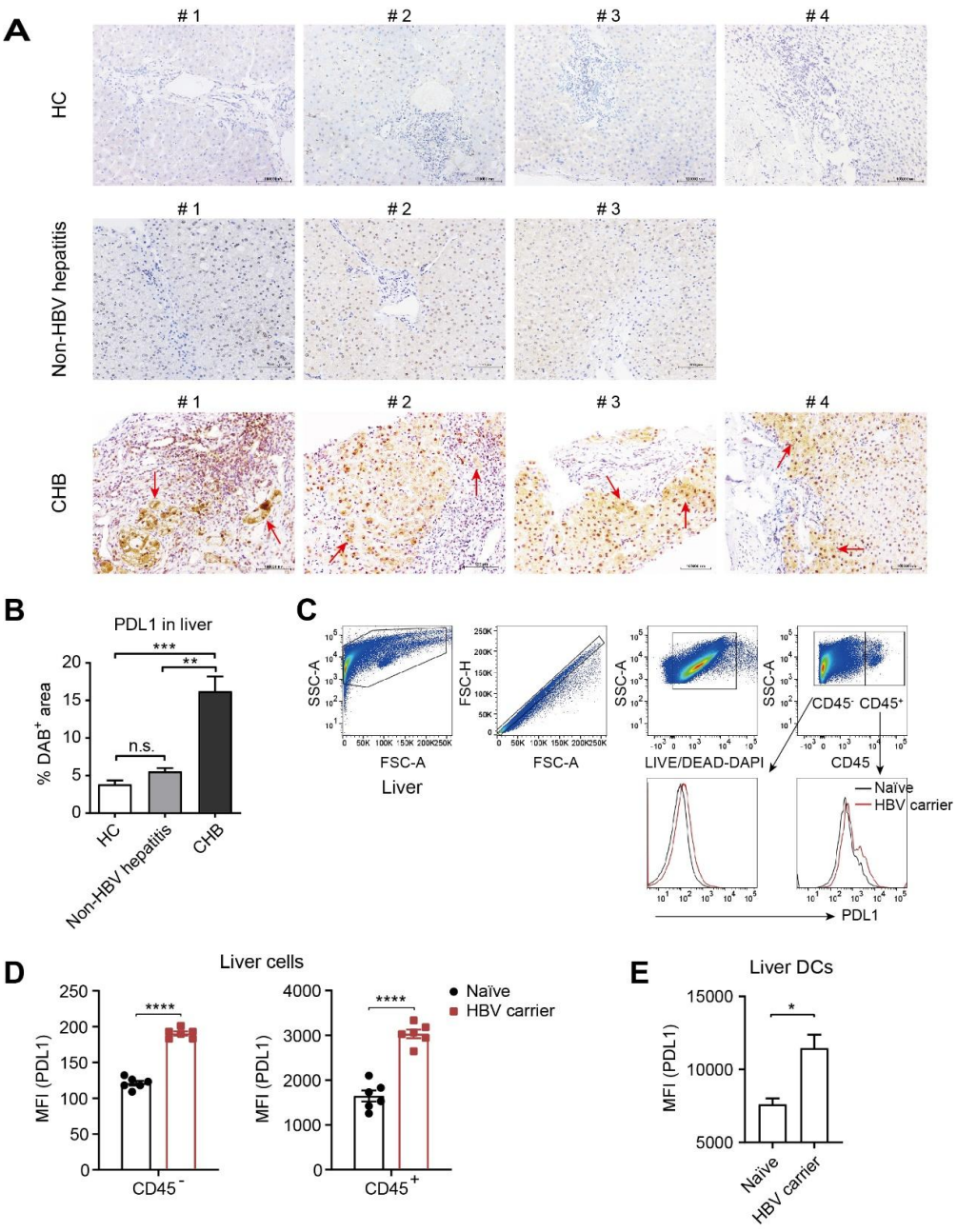

Supplementary Figure 1. Up-regulation of PDL1 in the liver of CHB patients and HBV carrier mice. (A) Immunohistochemical staining of PDL1 (× 200) in the liver of human healthy controls, non-HBV liver disease patients and CHB patients. Representative graphs of 3 to 4 samples in each group are shown. Arrows indicate the

representative PDL1 positive cells. Scale bars, 100 μm. (B) The percentage of the PDL1-staining positive area was quantified using ImageJ software (FIJI) (n = 6/HC, n = 3/non-HBV hepatitis, n = 7/CHB). (C) Gating strategy for the expression of PDL1 on $CD45^-$ cells and $CD45^+$ cells from HBV carrier mouse liver. (D) Liver tissues of naïve or HBV carrier mice (n = 6) were collected. PDL1 levels on $CD45^-$ cells and $CD45^+$ cells were evaluated by flow cytometry. (E) Liver tissues of naïve or HBV carrier mice (n = 3-7) were collected. PDL1 levels on hepatic DCs ($CD11c^+$MHC II^+) were evaluated by flow cytometry. Data are shown as the mean + SEM (B and E) or mean ± SEM (D) and are representative of at least two independent experiments. **P* < 0.05; ***P* < 0.01; ****P* < 0.001; *****P* < 0.0001. CHB, chronic hepatitis B; DAB, 3,3-diaminobenzidine tetrahydrochloride; DC, dendritic cell; HC, healthy controls; MFI, mean fluorescence intensity; n.s., not significant; PDL1, programmed death ligand 1.

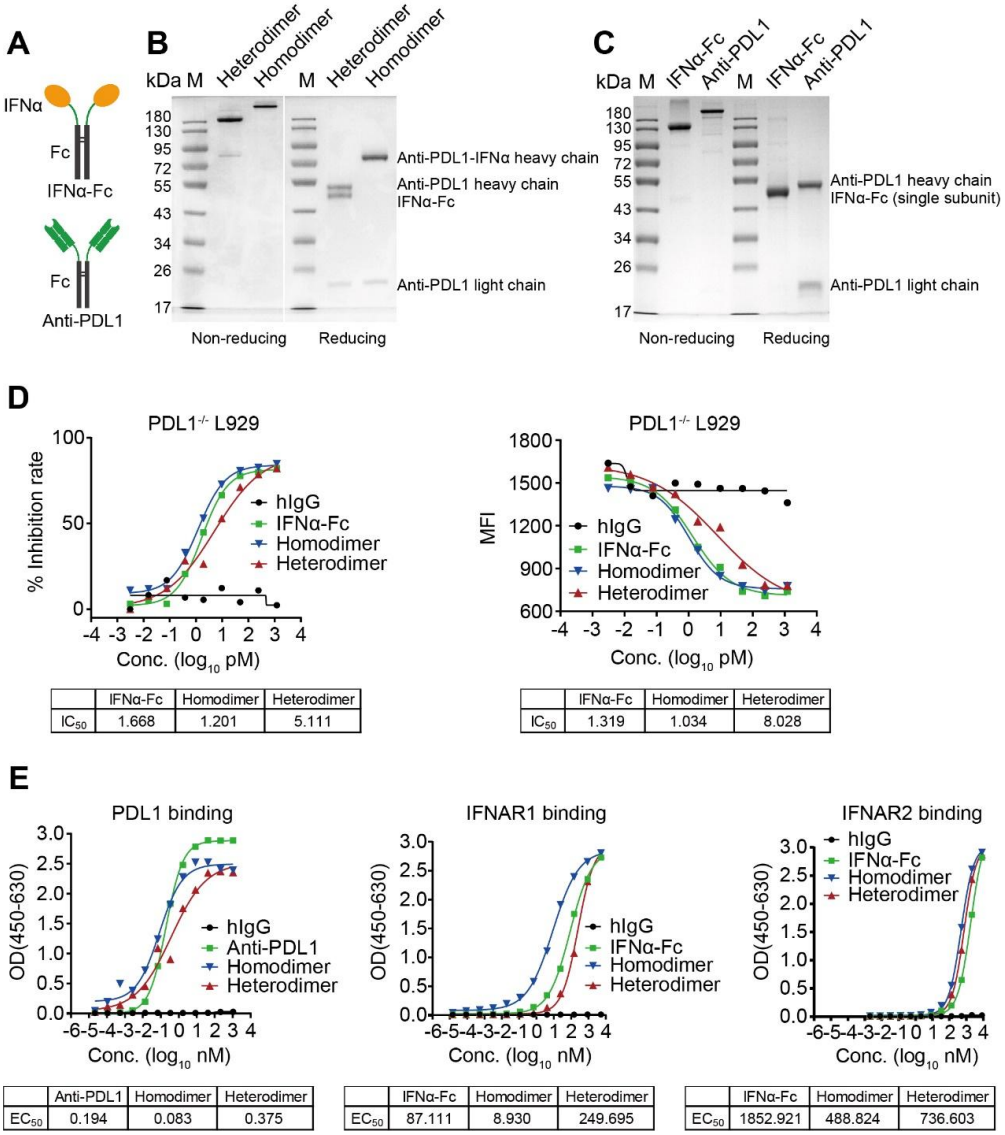

	IFNα-Fc	Homodimer	Heterodimer
IC_{50}	1.668	1.201	5.111

	IFNα-Fc	Homodimer	Heterodimer
IC_{50}	1.319	1.034	8.028

	Anti-PDL1	Homodimer	Heterodimer
EC_{50}	0.194	0.083	0.375

	IFNα-Fc	Homodimer	Heterodimer
EC_{50}	87.111	8.930	249.695

	IFNα-Fc	Homodimer	Heterodimer
EC_{50}	1852.921	488.824	736.603

Supplementary Figure 2. Biochemistry properties of fusion proteins. (A) Schematic structure of IFNα-Fc and anti-PDL1 fusion proteins. (B) Anti-PDL1-IFNα homodimer or heterodimer fusion protein was expressed in 293F cells and analyzed by gel electrophoresis after purification. (C) IFNα-Fc or anti-PDL1 fusion protein was expressed in 293F cells and analyzed by gel electrophoresis after purification. (D) The bioactivity of anti-PDL1-IFNα homodimer or heterodimer was measured by an antiviral infection

biological assay. PDL1$^{-/-}$ L929 cells were cultured with each protein (equimolar IFNα concentration, as determined by the single subunit) overnight before being infected with VSV-GFP. The percentage of GFP^{+} cells was measured by flow cytometry. The inhibition rate is normalized to the highest GFP^{+} percentage. The MFI of GFP^{+} was defined as virus replication intensity. (E) Binding curves of anti-PDL1-IFNα homodimer or heterodimer (equimolar anti-PDL1 or IFNα concentration, as determined by the single subunit) to the coated PDL1, IFNAR1 or IFNAR2 by ELISA. Panels B-E show representative of at least two independent experiments. EC_{50}, half-maximal effective concentration; ELISA, enzyme-linked immunosorbent assay; hIgG, human immunoglobulin G; IC_{50}, half-maximal inhibitory concentration; IFNAR, type I IFN receptor; M, molecular weight marker; MFI, mean fluorescence intensity; OD, optical density; PDL1, programmed death ligand 1.

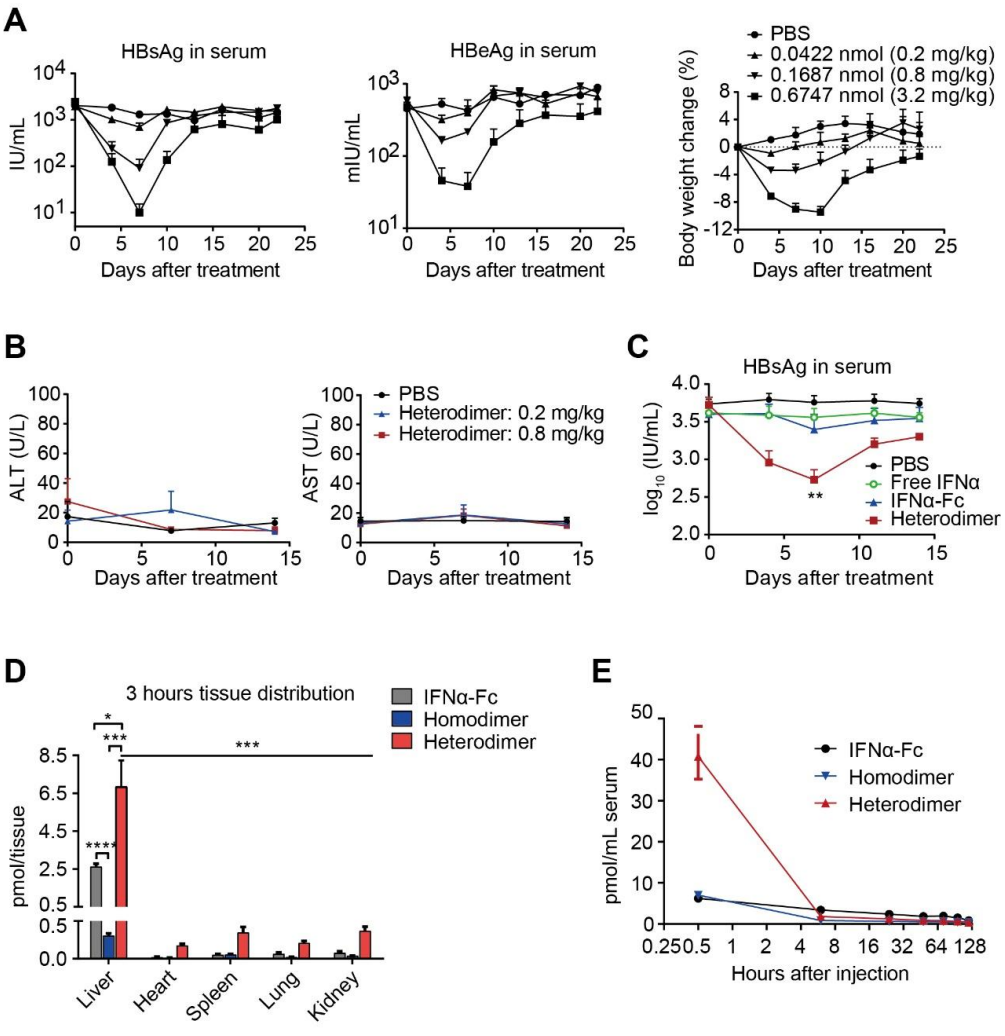

Supplementary Figure 3. Anti-PDL1-IFNα heterodimer presents more efficient liver targeting and lower toxicity. (A) Serum levels of HBsAg (left), HBeAg (middle), and body weight changes (right) of HBV carrier mice (n = 3) that received intravenous injections of anti-PDL1-IFNα heterodimer at the indicated doses on days 1 and 4. (B) HBV carrier mice (n = 5) were injected intravenously with anti-PDL1-IFNα heterodimer at the indicated doses on days 1 and 4. The sera were collected on days 0, 7 and 14. Glutamic–pyruvic transaminase (ALT) and glutamic–oxaloacetic transaminase (AST)

were measured following the manufacturer's instructions (Nanjing Jiancheng Bioengineering Institute, Nanjing, China). (C) HBV carrier mice (n = 3) were treated with equimolar IFNα (0.1687 nmol, as determined by the single subunit) on days 1 and 4. Serum levels of HBsAg were determined using ELISA. (D and E) HBV carrier mice (n = 6) were injected intravenously with a single dose (0.1687 nmol) IFNα-Fc, homodimer, or heterodimer. Tissues were collected, weighed, and homogenized at 3 hours after injection, and the concentrations of fusion proteins were measured by ELISA (D). Serum concentrations of fusion proteins at the indicated time points were measured by ELISA (E). Data are shown as the mean + SEM (A-D) or mean ± SEM (E) and are representative of at least two independent experiments (A-C) or are pooled from two independent experiments (D and E). $*P < 0.05$; $**P < 0.01$; $***P < 0.001$; $****P < 0.0001$. ELISA, enzyme-linked immunosorbent assay; HBeAg, hepatitis B e antigen; HBsAg, hepatitis B surface antigen; IU, international units; PBS, phosphate buffer saline.

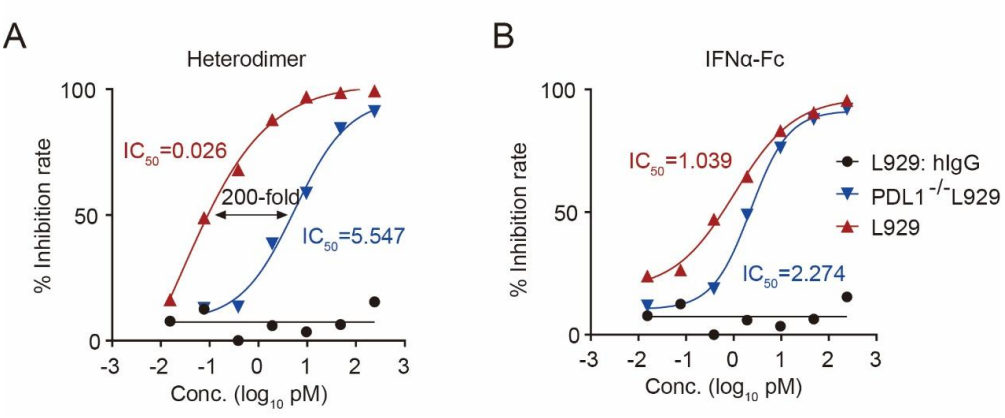

Supplementary Figure 4. Anti-PDL1-IFNα heterodimer exerts a more potent antiviral effect on PDL1-expressing L929 cells. (A and B) Antiviral activity of heterodimer (A) or IFNα-Fc (B) for inhibiting VSV-GFP infection in PDL1$^{-/-}$ L929 cells (blue symbols) or L929 cells (red symbols). Data are representative of at least two independent experiments. hIgG, human immunoglobulin G; IC_{50}, half-maximal inhibitory concentration; PDL1, programmed death ligand 1.

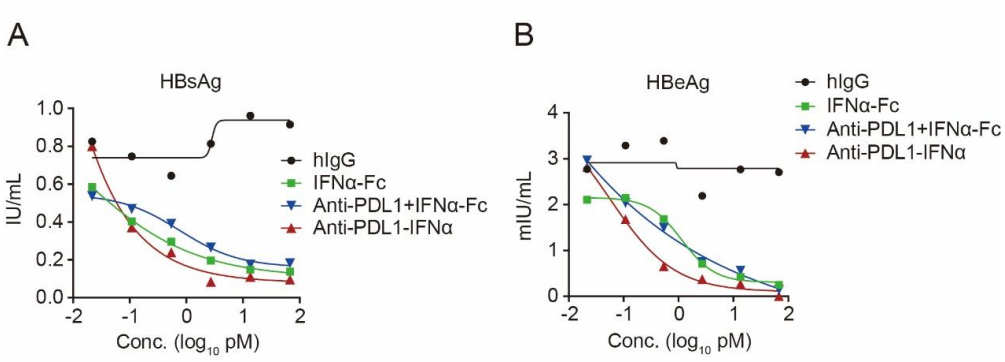

Supplementary Figure 5. Anti-PDL1-IFNα (human) heterodimer presents a synergistic anti-HBV effect on human hepatocytes. (A and B) HepG2-hNTCP cells were incubated with serial dilutions of anti-PDL1-IFNα (human) heterodimer, IFNα-Fc (human), or the mixture of IFNα-Fc (human) and anti-PDL1 (equimolar IFNα and anti-PDL1, as determined by the single subunit) at 37 °C overnight. Then, the cells were infected with 1×10^7 viral genome equivalents (vg) HBV and cultured for another 24 hours. The cells were washed with medium three times and maintained in PMM. Three days later, levels of HBsAg (A) and HBeAg (B) in the supernatant were detected by ELISA. Data are representative of at least two independent experiments. ELISA, enzyme-linked immunosorbent assay; HBeAg, hepatitis B e antigen; HBsAg, hepatitis B surface antigen; hIgG, human immunoglobulin G; IU, international units.

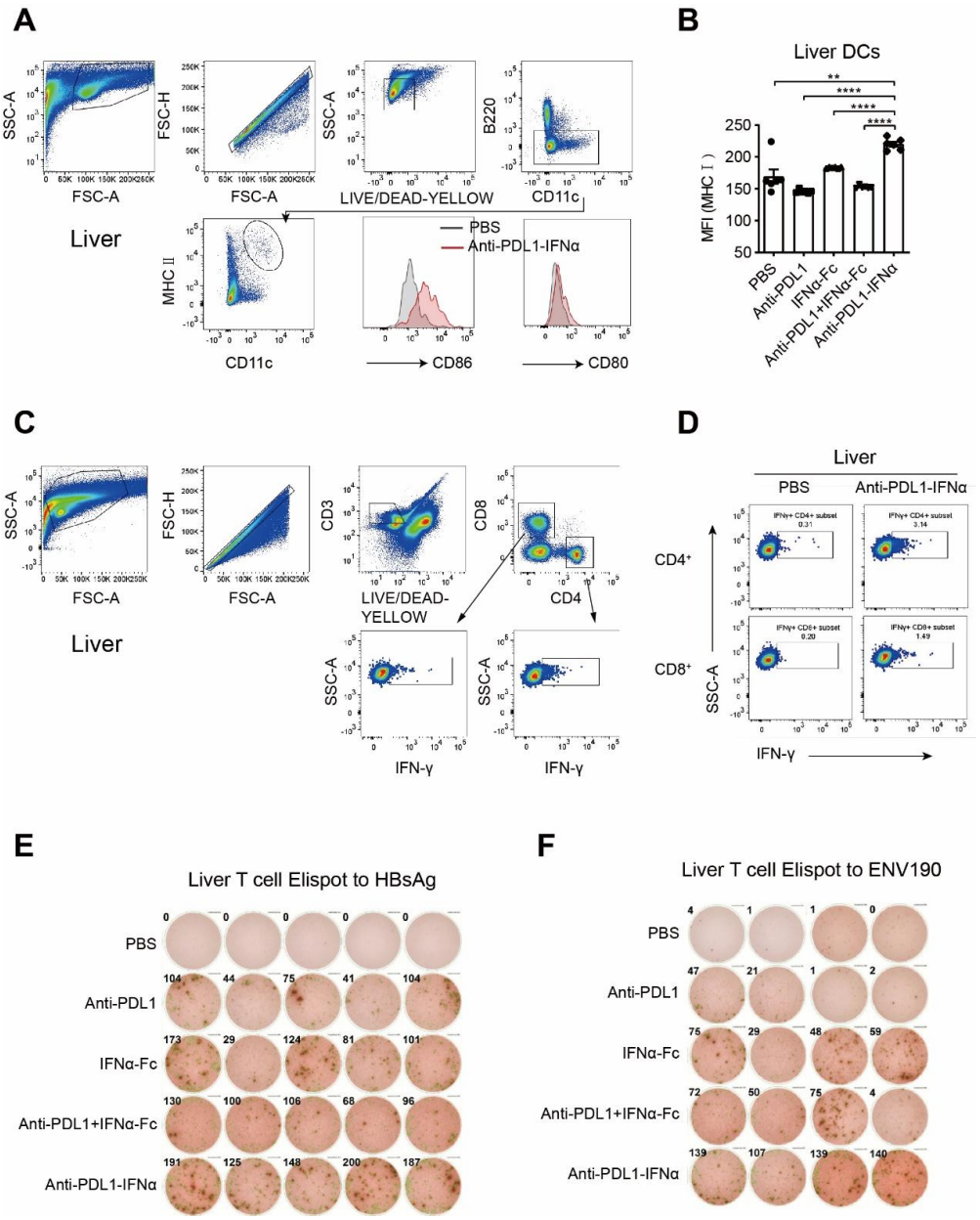

Supplementary Figure 6. Anti-PDL1-IFNα heterodimer improves the function of DCs for HBsAg-specific T cells in HBV carrier mice. (A) Gating strategy for the expression of CD86 and CD80 on DCs ($CD11c^+$ MHC II^+) from HBV carrier mouse liver. (B) HBV carrier mice (n = 6) were treated as described in Figure 3A. Hepatic mononuclear cells

were harvested on day 4. Flow cytometry was performed to analyze the expression of MHC I on DCs within liver. Data are shown as the mean ± SEM and are representative of at least two independent experiments. $^{**}P < 0.01$; $^{****}P < 0.0001$. (C and D) HBV carrier mice were treated as described in Figure 3A. Hepatic mononuclear cells were harvested on day 4 and stimulated with HBsAg (5 μg/mL; subtype ayw) in the presence of Brefeldin A (5 μg/mL) ex vivo. The frequencies of IFN-γ^+ cells among total $CD4^+$ or $CD8^+$ T cells within liver were determined by flow cytometry. Gating strategy for IFN-γ^+CD4^+ or IFN-γ^+CD8^+ T cells from HBV carrier mouse liver (C). A representative graph is shown (D). (E and F) For HBV-specific T cell Elispot assay (Figure 3E), HBV carrier mice were treated as described in Figure 3A. 5×10^5 hepatic mononuclear cells of each mouse were collected on day 4. HBV-specific T cell responses were tested by a T cell Elispot assay. Representative graphs are shown of two independent experiments. DC, dendritic cell; Elispot, enzyme-linked immunospot assay; MFI, mean fluorescence intensity; PBS, phosphate buffer saline.

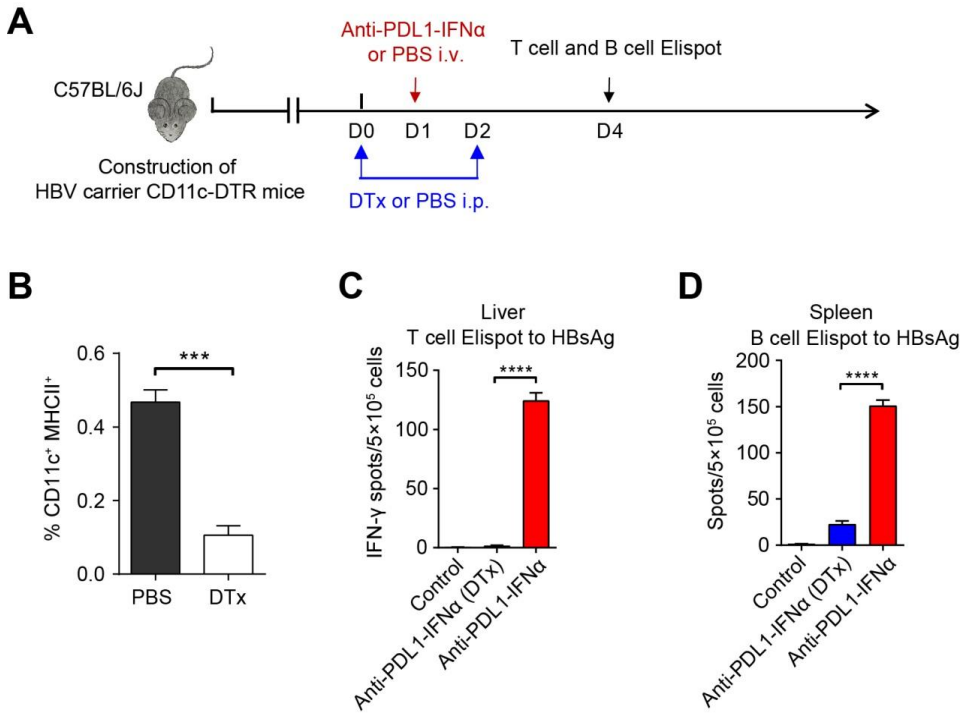

Supplementary Figure 7. Dendritic cells play essential roles in the anti-PDL1-IFNα heterodimer therapeutic approach. (A) HBV carrier CD11c-DTR mice were injected intraperitoneally with DTx (4 ng/g body weight) (Millipore, Darmstadt, Germany) or PBS on days 0 and 2, and a single dose (0.1687 nmol) of anti-PDL1-IFNα heterodimer treatment on day 1. Hepatic mononuclear cells and splenocytes were collected on day 4. (B) The percentage of DCs in the spleen of HBV carrier CD11c-DTR mice (n = 4) 24 hours after DTx or PBS injection. (C and D) HBsAg-specific T and B cells in the liver and spleen (n = 4) were measured by T cell and B cell Elispot assays, respectively. Data are shown as the mean + SEM. ***P < 0.001; ****P < 0.0001. DTx, diphtheria toxin; Elispot, enzyme-linked immunospot assay; i.p., intraperitoneal; i.v., intravenous.

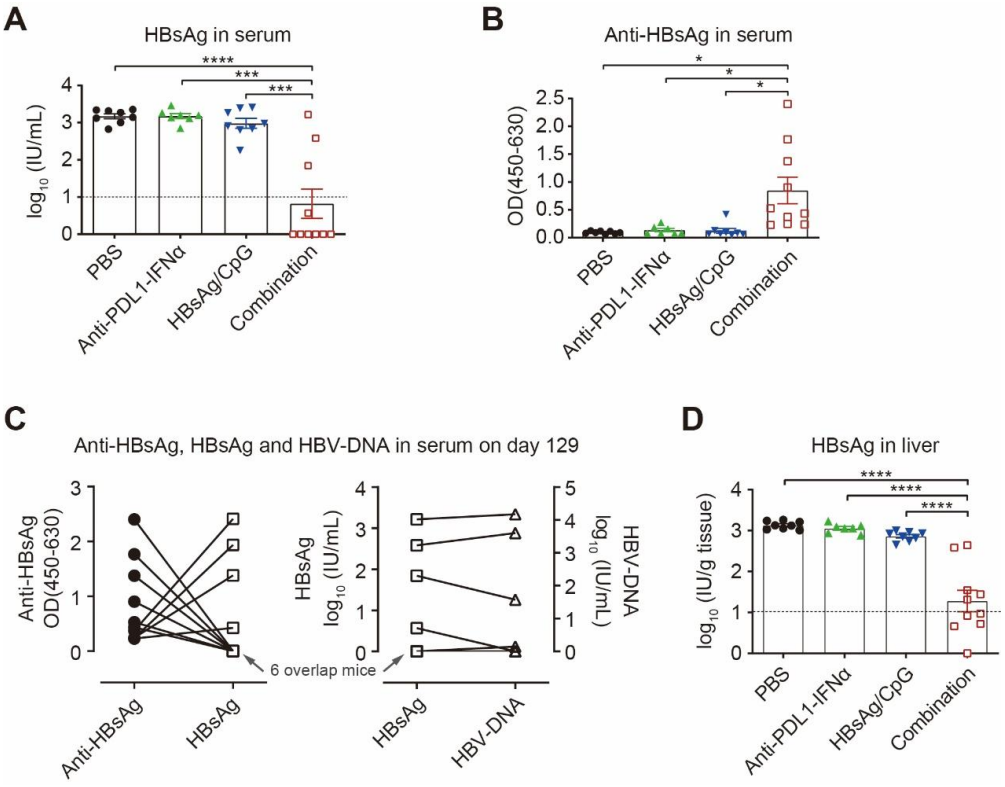

Supplementary Figure 8. HBsAg and anti-HBsAg levels of each mouse on day 129. (A and B) Serum levels of HBsAg (A) and ayw subtype-specific anti-HBsAg (B) of each mouse on day 129 in Figure 5B and C. (C) The correlation between anti-HBsAg and HBsAg and the correlation between HBsAg and HBV-DNA on day 129 in the combination therapy group (n = 10) were shown. (D) Liver tissues (n = 7-10) were harvested, weighed, and homogenized on day 129. Liver HBsAg levels were measured by ELISA. The detection limits in panels A and D are shown as dashed lines. Data are shown as the mean ± SEM (A, B, and D) (n = 7-10 mice per group from N = 2 independent experiments). **P* < 0.05; ****P* < 0.001; *****P* < 0.0001. CpG, cytosine–phosphate–guanine; ELISA, enzyme-linked immunosorbent assay; HBsAg, hepatitis B surface antigen; IU, international units; OD, optical density; PBS, phosphate buffer saline.

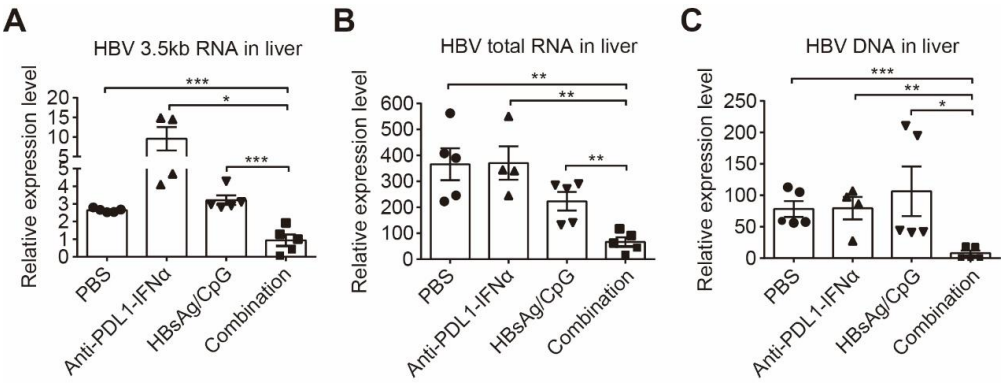

Supplementary Figure 9. Combination therapy can inhibit HBV replication in the liver. (A-C) HBV intermediate products HBV 3.5-kb RNA (A), HBV total RNA (B) and HBV-DNA (C) in the liver at the end of the experiment were measured with real-time PCR (n = 4-5). Data are shown as the mean ± SEM and are representative of at least two independent experiments. **P* < 0.05; ***P* < 0.01; ****P* < 0.001. CpG, cytosine–phosphate–guanine; PBS, phosphate buffer saline.

Supplementary Table 1. Clinical Characteristics of Study Cohort

	Age	HBsAg (IU/mL)	HBeAg (COI)	ALT (U/L)	AST (U/L)
HC (n = 6)	36.33±13.37	_*	_*	17.93±6.56	18.35±2.90
non-HBV (n = 3)	41.00±4.00	_*	_*	72.00±20.07	60.67±13.87
CHB (n = 7)	25.71± 12.27	15,412.07± 17,834.60	635.66± 668.66	98.14± 95.39	52.14± 33.75

Age, HBsAg, HBeAg, ALT and AST are shown as the mean ± SD. HC, healthy controls (liver transplantation donors); non-HBV, non-HBV liver disease patients (non-alcoholic fatty liver disease); CHB, chronic hepatitis B.

*HBsAg and HBeAg were negative.

416 Supplementary Table 2. Flow cytometry antibodies

Antibodies	Fluorochrome	Clone	Source
Anti-mouse CD45	AF700 or PerCP-Cy5.5	30-F11	eBioscience or BioLegend
anti-mouse CD3ε	FITC	145-2C11	eBioscience
anti-mouse CD4	PerCP-Cy5.5	RM4-5	eBioscience
anti-mouse CD8	APC or PE	53-6.7	eBioscience or BioLegend
anti-mouse IFN-γ	PE	XMG1.2	BioLegend
anti-mouse B220	BV 650	RA3-6B2	BioLegend
anti-mouse CD11c	APC	N418	Invitrogen
anti-mouse MHC II	FITC or AF700	M5/114.15.2	eBioscience
anti-mouse MHC I	PerCP-eFluor® 710	SF1-1.1.1	eBioscience
anti-mouse CD80	FITC	16-10A1	Tonbo
anti-mouse CD86	PE	GL1	eBioscience
anti-mouse CD11b	PerCP-Cy5.5	M1/70	eBioscience
anti-mouse F4/80	PE	BM8	eBioscience
anti-mouse Gr-1	eF450 or AF488	RB6-8C5	Invitrogen
anti-mouse CD19	APC	MB19-1	eBioscience
anti-mouse PDL1	PE-Cy7	10F.9G2	BioLegend

417